

Volume 4  
Issue 1  
July 2015

ISSN 1857-839X

**SJCE**

**SCIENTIFIC  
JOURNAL  
OF CIVIL  
ENGINEERING**



SS CYRIL AND METHODIUS UNIVERSITY  
**FACULTY OF CIVIL ENGINEERING**



9 785056 235095





## **EDITORIAL - Preface to Volume 4 Issue 1 of the Scientific Journal of Civil Engineering (SJCE)**

### **Darko Moslavac EDITOR – IN - CHIEF**

---

Dear Readers,

Scientific Journal of Civil Engineering was established in December 2012. This effort, led by Faculty of Civil Engineering (FCE) – Skopje creates opportunities for staff and postgraduate students at FCE to publish the results of their research activities for the general scientific and professional community.

We would also like to address to our scientific colleagues from abroad to participate in the editorial board of the SJCE to expand the scope of the journal with assistance of our partners from abroad, especially those with which Faculty of Civil Engineering – Skopje has conducted long – term research and maintains working contacts.

SJCE is published bi-annually and is available online at FCE web site ([www.gf.ukim.edu.mk](http://www.gf.ukim.edu.mk)).

It is my pleasure to introduce the First Issue of VOLUME 4 of the Scientific Journal of Civil Engineering (SJCE).

At the beginning of the fourth year of publication of our journal we are now able to think with justification about the realization of the ideas which led us to launch the journal, the positive results achieved together with authors and readers, but also about new challenges for the future.

This issue includes 5 articles in the field of: long-term effects on concrete elements under variable load, cadastre services

oriented toward administering with agriculture land concessions, mathematical models for analysis of water hammer in the water supply network, analysis of reinforced beams, impact of ground vibrations induced by pile driving and preparation of landslide susceptibility maps using gis.

It's our honour to publish several articles that presents the results from research conducted in the doctoral dissertations of a few of our young colleagues. Special gratitude to all authors whose papers are published in this issue.

We continue to invite all researchers, practitioners and members of the academic community to contribute through their articles to the development and maintenance of the quality of the SJCE journal. We are particularly pleased to publish the results of research, best practice, case studies, ideas for solutions of complex problems, proposals of innovations and the results of experience on important projects.

Sincerely Yours,

Prof. Ph.D. Darko Moslavac

July, 2015



## Impressum

### FOUNDER AND PUBLISHER

Faculty of Civil Engineering -Skopje  
Partizanski odredi 24, 1000 Skopje

### EDITORIAL OFFICE

Faculty of Civil Engineering -Skopje  
Partizanski odredi 24, 1000 Skopje  
Rep. of Macedonia tel. +389 2  
3116 066; fax. +389 2 3118 834  
Email:  
prodekan.nauka@gf.ukim.edu.mk

### EDITOR IN CHIEF

Prof. Ph.D. **Darko Moslavac**  
University Ss. Cyril and Methodius  
Faculty of Civil Engineering -Skopje  
Partizanski odredi 24, 1000 Skopje  
Rep. of MACEDONIA tel. +389 71  
368 372; Email:  
[moslavac@gf.ukim.edu.mk](mailto:moslavac@gf.ukim.edu.mk)

**ISSN: 1857-839X**

### EDITORIAL BOARD

Prof. Ph.D. **Darko Moslavac**  
University Ss. Cyril and Methodius,  
Rep. of Macedonia  
Prof. dr. sc. **İbrahim Gurer**  
Gazi University, Turkey  
Prof. dr **Miodrag Jovanovic**  
University of Belgrade, Rep. of  
Serbia  
Em.O.Univ.Prof. Dipl.-Ing.  
Dr.h.c.mult. Dr.techn. **Heinz Brandl**  
Vienna University of Technology,  
Austria  
Prof. dr. sc. **Zalika Črepinšek**  
University of Ljubljana, Slovenia  
Prof.dr.ir. **J.C. Walraven**  
Delft University of Technology,  
Netherland  
univ.dipl.ing.gradb. **Viktor Markelj**  
University of Maribor, Slovenia  
PhD, Assoc. Prof. **Jakob Likar**  
University of Ljubljana, Slovenia  
PhD,PE,CE **Davorin KOLIC**  
ITA Croatia  
Prof. dr. sc. **Stjepan Lakušić**  
University of Zagreb, Croatia  
**Marc Morell**  
Institut des Sciences de l'Ingénieur  
de Montpellier, France  
Prof. Ph.D. **Miloš Knežević**  
University of Montenegro  
Prof. Ph.D. **Milorad Jovanovski**  
University Ss. Cyril and Methodius,  
Rep. of Macedonia  
Prof. Ph.D. **Cvetanka Popovska**  
University Ss. Cyril and Methodius,  
Rep. of Macedonia  
Prof. Ph.D. **Ljupco Lazarov**  
University Ss. Cyril and Methodius,  
Rep. of Macedonia  
Prof. Ph.D. **Goran Markovski**  
University Ss. Cyril and Methodius,  
Rep. of Macedonia

Prof. Ph.D. **Zlatko Srbinovski**  
University Ss. Cyril and Methodius,  
Rep. of Macedonia  
Prof. Ph.D. **Elena Dumova  
Jovanovska**  
University Ss. Cyril and Methodius,  
Rep. of Macedonia

### ORDERING INFO

**SJCE** is published semiannually.  
All articles published in the journal  
have been reviewed.

Edition: 200 copies

### SUBSCRIPTIONS

Price of a single copy: for  
Macedonia (500 den); for abroad  
(10 EUR + shipping cost).

### BANKING DETAILS (MACEDONIA)

Narodna banka na RM  
Account number:  
160010421978815  
Prihodno konto 723219  
Programa 41

### BANKING DETAILS (INTERNATIONAL)

Corespond bank details:  
Deutsche Bundesbank Zentrale  
Address: Wilhelm Epstein strasse  
14 Frankfurt am Main, Germany  
SWIFT BIC: MARK DE FF  
Bank details:  
National Bank of the Republic of  
Macedonia  
Address: Kompleks banki bb 1000  
Skopje Macedonia  
SWIFT BIC: NBRM MK 2X  
IBAN: MK 07 1007 0100 0036 254  
Name: Gradezen fakultet Skopje

### PRINT

Printing house SANIKO




# CONTENT

---

Goce Taseski MATHEMATICAL MODEL FOR ANALYSIS OF WATER HAMMER IN THE WATER SUPPLY NETWORK	7
Darko Nakov, Goran Markovski, Toni Arangjelovski, Peter Mark DETERMINATION OF THE COEFFICIENT $\psi_2$ TO DEFINE LONG-TERM EFFECTS ON CONCRETE ELEMENTS UNDER VARIABLE LOAD	15
Mile R. Mihajlov CONTRIBUTION TO THE ANALYSIS OF REINFORCED BEAMS - PART I	23
Gjorgjiev Vanco, Gjorgjiev Gjorgji CADASTRE SERVICES ORIENTED TOWARD ADMINISTERING WITH AGRICULTURE LAND CONCESSIONS	37
Igor Peševski , Milorad Jovanovski, Jovan Br. Papić, Luka Jovičić PREPARATION OF LANDSLIDE SUSCEPTIBILITY MAPS USING GIS, RECENT CASE STUDY IN R.MACEDONIA	47





Become a student of the Faculty of Civil Engineering and a part of the impetus that creates and build the world! Step in the world of the successful people, because even the longest roads start with the first step. You will spend a part of your youth with us, and the youth is expensive to be misspent in vain. Your choice is an exceptional profession, for people who do believe in themselves, profession that requires prompt and courageous decisions. This profession will provide you with great privileges: your actions will remain an eternal record in the space and in the time being.

- STRUCTURAL ENGINEERING
- HYDRO-TECHNICAL ENGINEERING
- ROADS AND RAILWAYS ENGINEERING
- GEODESY
- GEOTECHNICAL ENGINEERING



## MATHEMATICAL MODEL FOR ANALYSIS OF WATER HAMMER IN THE WATER SUPPLY NETWORK

### AUTHOR

**Goce Taseski**

Ph.D. Assistant

Ss. Cyril and Methodius University

Faculty of Civil Engineering – Skopje

[taseski@gf.ukim.edu.mk](mailto:taseski@gf.ukim.edu.mk)

Water supply systems as complex systems commonly in practice are hydraulically analyzed with superior quasi steady regime of flow. In general, the hydraulic regime in all water supply systems is unsteady but very often during the design the hypothesis of quasi steady regime is justified. However, in water supply systems equipped with pump and turbine plants, exclusion and inclusion thereof leads to a state of transitional hydraulic regimes caused by abrupt opening or closing of the valves, then to occurrence of defects. In such transient regimes occurs the phenomenon of water hammer that causes abrupt increase or decrease of the flow and pressure on parts or the whole water supply system. The water supply systems in such transient flows should hydraulically be analyzed with the basic equations for unsteady flow.

This paper develops an individual mathematical model HTM for analysis of water networks in conditions of unsteady flow, i.e. with the mathematical model the characteristics of the water hammer can be seen in the closed systems for transport of water under pressure. The verification of the results of its own mathematical model is made with proprietary software to analyze the water hammer. (HAMMER).

**Keywords:** water supply network, mathematical model, water hammer, method of characteristics.

### INTRODUCTION

Water supply systems [3] are complex systems that can be composed of: objects which are capturing the water, objects that are used for improvement of the water quality, water intakes that may be gravity or pump, objects to change the pressure, valves, tanks and home plumbing. Such complexity of the water supply systems is leading to water flow under pressure where the speed and pressure change over time - unsteady flow of water.

The analysis of the water hammer occurrence [6] in the water networks in past practice has not received the attention it deserves as in the design phase of such systems and in

managing them. In the past practice, the hydraulic analyses of water supply systems were conducted under the assumption for quasi steady regime of flow. It is understood that in reality the water flow in the water supply system is not in a steady regime but in an unsteady regime. The main reasons for such hydraulic analysis is due to the elaborateness and complexity of the mathematical solution to the problem, where from the designer its required not only education and good knowledge of the water hammer phenomenon but knowledge in the field of computer programming. For these reasons in the past practice the calculating of the water hammer by complex systems under pressure such as the water supply systems was done by simplifying the system and at the same time the designer relies on hitherto experience.

With the emergence of calculating machines and the development of program technologies in the recent decades it is noticeable an intensive development of mathematical models for complex flow as the water hammer in complex systems [12]. However, to date there is still no exact model for analysis of the hydraulic model of the water supply systems mainly because of their complexity and the fact that in these systems there is no identical system i.e. any water supply system is a "unique" system. Accordingly, in addition this paper presents the development of a mathematical model that is applicable to the analysis of the water hammer in the water supply systems.

## BASIC EQUATIONS FOR WATER HAMMER

According Wylie [5] (1993), the water hammer is defined as the hydraulic variable occurrence of flow, which causes an increase of overpressure in a pipeline system. The water hammer can be generated by certain operational measures such as: opening or closing of the valve, turning the pumps on or off, abrupt cracking of the tube etc.

Starting points in the mathematical description of the water hammer [9] are the basic laws in the mechanics of fluids:

- Law of maintaining the amount of movement and
- Law of maintaining weight.

Satisfying these basic principles for conservation/maintenance comes to the

dynamic equation and the equation of continuity.

The final form of the dynamic equation for unsteady flow in closed systems under pressure:

$$\frac{\partial V}{\partial t} + V \frac{\partial V}{\partial x} + g \frac{\partial \Pi}{\partial x} + \frac{\lambda}{2D} V |V| = 0 \quad (1)$$

The convective acceleration  $V \partial V / \partial x$  or acceleration along the pipe is significantly lower compared to the local acceleration  $\partial V / \partial t$  or acceleration over time, so mostly that convective acceleration is overlooked and the dynamic equation is written:

$$\frac{\partial V}{\partial t} + g \frac{\partial \Pi}{\partial x} + \frac{\lambda}{2D} V |V| = 0 \quad (2)$$

Assuming that the density of the fluid changes very little in terms of piezometric height ( $\rho = \text{const}$ ), the equation of continuity gets the following form:

$$V \frac{\partial \Pi}{\partial x} + \frac{\partial \Pi}{\partial t} - V \sin \alpha + \frac{a^2}{g} \frac{\partial V}{\partial x} = 0 \quad (3)$$

Where  $a$  is the speed of propagation of the pressure wave and it is determined by the ratio of compression of the fluid and the module of elasticity of the tube:

$$a = \sqrt{\frac{K}{\rho \left( 1 + \frac{K D}{E e} c_1 \right)}} \quad (4)$$

The coefficient  $c_1$  depends of the pipe anchorage and is equal to:

- ✓  $c_1 = 1 - \mu/2$  – pipe anchorage only at the upstream
- ✓  $c_1 = 1 - \mu/2$  – pipe anchorage throughout against axial movement
- ✓  $c_1 = 1$  – pipe anchorage with expansion joints throughout

## METHOD OF CHARACTERISTICS FOR SOLVING BASIC EQUATIONS OF WATER HAMMER

With the method of characteristics [15] the basic partial differential equations which are not integrable in closed form, are transformed into ordinary differential equations which have a solution in a closed form. The basic



equations, the equation of continuity and the dynamic equation can be designated with  $L_1$  и  $L_2$ :

$$L_1 = g \frac{\partial \Pi}{\partial x} + \frac{\partial V}{\partial t} + V \frac{\partial V}{\partial x} + \frac{\lambda}{2D} V |V| = 0 \quad (5)$$

$$L_2 = \frac{\partial \Pi}{\partial t} + V \frac{\partial \Pi}{\partial x} + \frac{a^2}{g} \frac{\partial V}{\partial x} - g \sin \alpha = 0 \quad (6)$$

These linear equations can be combined as follows:

$$L = L_1 + \chi L_2 \quad (7)$$

The two dependent variables, the speed  $V$  and the pressure  $\Pi$  are in a function from the position and time,  $V=V(x,t)$  и  $\Pi=\Pi(x,t)$ . The material statements of these dependent variables are total accelerations which are determined by the convective and local acceleration:

$$\frac{d\Pi}{dt} = \frac{\partial \Pi}{\partial x} \frac{dx}{dt} + \frac{\partial \Pi}{\partial t} \quad (8)$$

$$\frac{dV}{dt} = \frac{\partial V}{\partial x} \frac{dx}{dt} + \frac{\partial V}{\partial t} \quad (9)$$

Comparing the expression of the convective acceleration of equation (7) to those of equations (8) and (9), follows:

$$\frac{dx}{dt} = V + \frac{g}{\chi} = V + \frac{\chi a^2}{g} \quad (10)$$

Then equation 7 is written:

$$\chi \frac{d\Pi}{dt} + \frac{dV}{dt} + \frac{\lambda}{2D} V |V| - \chi g \sin \alpha = 0 \quad (11)$$

The solution of equation 11 is:

$$\chi = \pm \frac{g}{a} \quad (12)$$

$$\frac{dx}{dt} = V \pm a \quad (13)$$

From the previous equation it can be concluded that it's about two families of curves that are practically straight lines, where the speed of propagation is constant and many times faster than the basic flow, so the system of two partial differential equations are transformed into system of ordinary four differential equations which are marked with a  $C+$  and  $C-$  and determine straight lines:

$$\left. \begin{aligned} \frac{d\Pi}{dt} + \frac{a}{g} \frac{dV}{dt} + \frac{\lambda}{2D} V |V| - V \sin \alpha &= 0 \\ \frac{dx}{dt} &= V + a \end{aligned} \right\} C^+ \quad (14)$$

$$\left. \begin{aligned} -\frac{d\Pi}{dt} + \frac{a}{g} \frac{dV}{dt} + \frac{\lambda}{2D} V |V| + V \sin \alpha &= 0 \\ \frac{dx}{dt} &= V - a \end{aligned} \right\} C^- \quad (15)$$

## NUMERICAL MODEL

Figure 1 shows discretization of the physical system in a numerical network with computing steps  $\Delta x$  and  $\Delta t$  where the solutions are obtained at the intersection of the positive and negative lines of characteristics [8], [9], [10], [11].

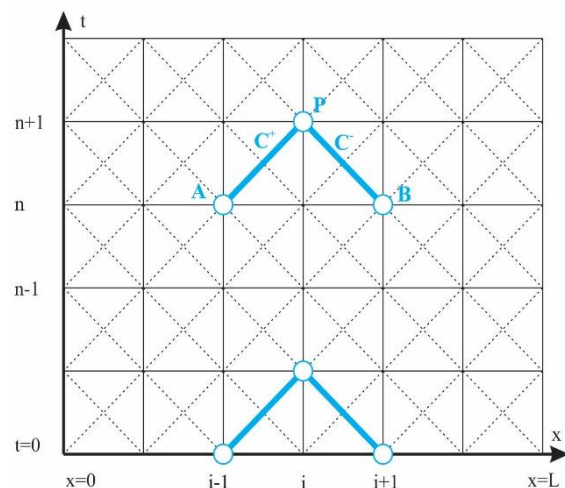


Figure 1. Numerical network for the method of characteristics.

According the given numerical network, equations (14) and (15) can be written as follows:

$$\frac{d}{dt} \left( \Pi \pm \frac{a}{g} V \right) + \lambda \frac{a}{D} \frac{V |V|}{2g} \mp V \sin \alpha = 0 \quad (16)$$

The previous equation can be integrated along the positive and negative characteristics, i.e. along the length of the lines  $AP$  and  $BP$ , as follows:

$$\int_{tA}^{tP} \frac{d}{dt} \left( \Pi + \frac{a}{g} V \right) dt + \int_{tA}^{tP} \left( \lambda \frac{a}{D} \frac{V |V|}{2g} - V \sin \alpha \right) dt = 0 \quad (17)$$

$$\int_{tB}^{tP} \frac{d}{dt} \left( \Pi - \frac{a}{g} V \right) dt + \int_{tB}^{tP} \left( \lambda \frac{a}{D} \frac{V |V|}{2g} + V \sin \alpha \right) dt = 0 \quad (18)$$

After integration, equations of positive and negative characteristic are written:

$$\frac{\Pi_P - \Pi_A}{\Delta t} + \frac{a}{g} \frac{V_P - V_A}{\Delta t} + \frac{\lambda a}{2gD} V_A |V_A| - V_A \sin \alpha = 0$$

$$\frac{\Pi_P - \Pi_B}{\Delta t} - \frac{a}{g} \frac{V_P - V_B}{\Delta t} + \frac{\lambda a}{2gD} V_B |V_B| - V_B \sin \alpha = 0$$

If it is known that the hydraulic analysis is important to determine the change in the flow and height position of the hydrodynamic line in any section along the pipe and at a specified interval, additional approximating is introduced that the cross-section of the pipe throughout its length is constant and if it is known that the average speed can be determined by the equation  $V=Q/A$ , the previous equations knowing the numerical network can be written in the following form:

$$\Pi_i^{n+1} - \Pi_{i-1}^n + \frac{a}{gA} (Q_i^{n+1} - Q_{i-1}^n) + \frac{\lambda \Delta x}{2gDA^2} Q_{i-1}^n |Q_{i-1}^n| - \frac{\Delta t}{A} Q_{i-1}^n \sin \alpha = 0 \quad (19)$$

$$\Pi_i^{n+1} - \Pi_{i+1}^n - \frac{a}{gA} (Q_i^{n+1} - Q_{i+1}^n) - \frac{\lambda \Delta x}{2gDA^2} Q_{i+1}^n |Q_{i+1}^n| - \frac{\Delta t}{A} Q_{i+1}^n \sin \alpha = 0 \quad (20)$$

If:

$$B = \frac{a}{gA} \quad \text{and} \quad M = \frac{\lambda \Delta x}{2gDA^2}$$

Using the previous equations, for the pressure, i.e. for the height position of the hydrodynamic line, it can be written:

$$\Pi_i^{n+1} = \Pi_{i-1}^n - B(Q_i^{n+1} - Q_{i-1}^n) - MQ_{i-1}^n |Q_{i-1}^n| + \frac{\Delta t}{A} Q_{i-1}^n \sin \alpha = 0 \quad (21)$$

$$\Pi_i^{n+1} = \Pi_{i+1}^n + B(Q_i^{n+1} - Q_{i+1}^n) + MQ_{i+1}^n |Q_{i+1}^n| + \frac{\Delta t}{A} Q_{i+1}^n \sin \alpha = 0 \quad (22)$$

If the parameters of flow are known in the time interval (n), then we get:

$$\Pi_i^{n+1} = CP - BQ_i^{n+1} \quad (23)$$

$$\Pi_i^{n+1} = CM + BQ_i^{n+1} \quad (24)$$

Where:

$$CP = \Pi_{i-1}^n + BQ_{i-1}^n - MQ_{i-1}^n |Q_{i-1}^n| + \frac{\Delta t}{A} Q_{i-1}^n \sin \alpha$$

$$CM = \Pi_{i+1}^n - BQ_{i+1}^n + MQ_{i+1}^n |Q_{i+1}^n| + \frac{\Delta t}{A} Q_{i+1}^n \sin \alpha$$

In the previous equations the article which include the slope of the pipes ( $\sin \alpha$ ) is very small and often overlooked, so the equations (25) and (26) are written:

$$CP = \Pi_{i-1}^n + BQ_{i-1}^n - MQ_{i-1}^n |Q_{i-1}^n| \quad (25)$$

$$CM = \Pi_{i+1}^n - BQ_{i+1}^n + MQ_{i+1}^n |Q_{i+1}^n| \quad (26)$$

From equations (25) and (26) is obtained a basic equation of the characteristics for determining the elevation of the hydrodynamic line:

$$\Pi_i^{n+1} = \frac{CP + CM}{2} \quad (27)$$

Knowing the piezometric height ( $\Pi_i$ ) in the time period ( $n+1$ ), the flow ( $Q_i$ ) is determined by equations (25) and (26).

## BOUNDARY CONDITIONS

The conditions of the flow that govern within the boundary of the system under pressure – the water supply system are defined as boundary conditions. Their definition is of crucial importance for getting the solution at the points in the system. Follow-on are the most common cases of boundary conditions encountered in the water supply systems [2].

### ✓ Serial connection of two pipes in a junction

$$\text{Pressure: } \Pi_{1,N}^{n+1} = \Pi_{2,1}^{n+1} = \Pi^{n+1}$$

$$\text{Flow: } Q_{1,N}^{n+1} = Q_{2,1}^{n+1} = Q^{n+1} = \frac{CP_1 - CM_2}{B_1 + B_2}$$

### ✓ Connection of more pipes in a junction

$$\text{Pressure: } \Pi^{n+1} = \Pi_{1,N}^{n+1} = \Pi_{2,1}^{n+1} = \Pi_{3,1}^{n+1} = \Pi_{4,1}^{n+1}$$

$$\Pi^{n+1} = \frac{CP_1 / B_1 + CM_2 / B_2 + CM_3 / B_3 + CM_4 / B_4}{1 / B_1 + 1 / B_2 + 1 / B_3 + 1 / B_4}$$

$$\text{Flow: } -Q_{1,N}^{n+1} = \frac{\Pi^{n+1}}{B_1} - \frac{CP_1}{B_1}; \quad Q_{2,1}^{n+1} = \frac{\Pi^{n+1}}{B_2} - \frac{CM_2}{B_2}$$

$$Q_{3,1}^{n+1} = \frac{\Pi^{n+1}}{B_3} - \frac{CM_3}{B_3}; \quad Q_{4,1}^{n+1} = \frac{\Pi^{n+1}}{B_4} - \frac{CM_4}{B_4}$$



✓ **Reservoir at the end of pipeline**

Pressure:  $\Pi_1^{n+1} = \Pi_R$

Flow:  $Q_1^{n+1} = \frac{(\Pi_1^{n+1} - CM)}{B}$

✓ **Valve at the end of the pipeline**

Pressure:  $\Pi_1^{n+1} = CP - BQ_N^{n+1}$

Flow:

$Q_N^{n+1} = -B \cdot C_1 + \sqrt{(B \cdot C_1)^2 + 2C_1(CP - Z_Z)}$

$C_1 = g \frac{A_C^2}{\xi_Z}$

✓ **Valve at the middle of the pipeline**

Pressure:

$\Pi_{1,N}^{n+1} = CP_1 - B_1 Q_{1,N}^{n+1} ; \Pi_{2,1}^{n+1} = CM_2 - B_2 Q_{2,1}^{n+1}$

$CP_1 - B_1 Q^{n+1} - CM_2 - B_2 Q^{n+1} - C_1 Q^{n+1} |Q^{n+1}| = 0$

If the condition is completed  $CP_1 - CM_2 > 0$  than follows:

Flow:

$Q^{n+1} = \frac{-(B_1 + B_2) + \sqrt{(B_1 + B_2)^2 + 4C_1(CP_1 - CM_2)}}{2C_1}$

If  $CP_1 - CM_2 < 0$  than follows:

Flow:

$Q^{n+1} = \frac{(B_1 + B_2) - \sqrt{(B_1 + B_2)^2 - 4C_1(CP_1 - CM_2)}}{2C_1}$

**Development of the mathematical model**

The mathematical model HTM [1] is set so that the water supply system only in unsteady regime is analyzed. The steady regime that is governing in the system before the emergence of unsteadiness is taken over of readymade modern software packages for the analysis of systems under pressure, such as EPANET, WaterCAD, WaterGEMS etc. In particular, in the development of the mathematical model HTM the initial conditions of the course – steady conditions are taken from the software package WaterGEMS.

For the development of the mathematical model HTM accounting scheme is used at a

zoned gravity water supply system with spread water system, where the water from the source of water - tapping (R) is distributed in the upper height zone and the excess water i.e. the needs of water for the lower zone are filling the reservoir (T) for the lower zone.

The choice of such calculation scheme is made to analyze the phenomenon of the water hammer in a complex system with a gravity intake and a closure at the end of the primary pipeline. This accounting scheme is practically equivalent to the model of a simple system - reservoir and pipeline which eventually have closure at the end, figure 3.

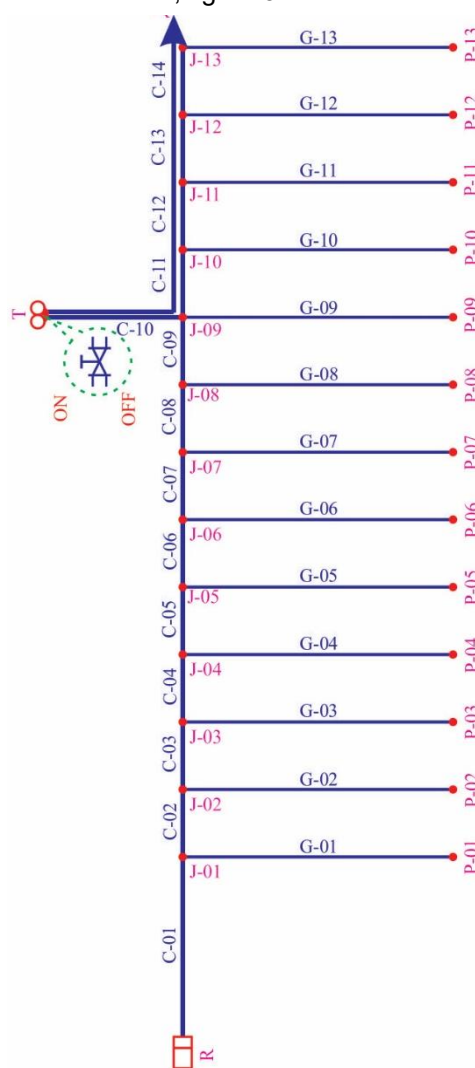


**Figure 3.** Calculation scheme for the development of the mathematical model HTM

The flow-through amount of water by movements in a steady regime of flow when the float valve is opened and closed are displayed on the figure 4.

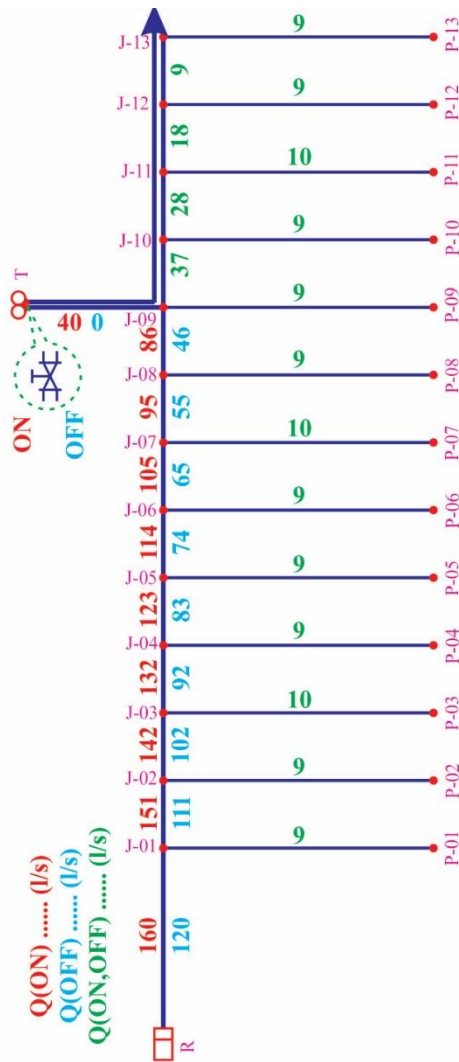


**Figure 4.** Flow amount of water in a steady regime of flow.

In Table 1 are given characteristics of the pipeline material and the water characteristics, while the geometric characteristics of pipelines and elevation of the junction are given in Table 2.

**Table 1.** Material characteristics of pipelines and water as fluid

Characteristics	Value
DUCTIL PIPES	
Young modulus of elasticity	170 GPa
Poisson factor	0.28
FLUID – WATER	
Temperature	20°C
Density	998 kg/m <sup>3</sup>
Modulus of elasticity	2.19 GPa
Kinematic viscosity	1.01×10 <sup>-6</sup> m <sup>2</sup> /s

**Table 2.** Geometric characteristics of the system for the first scenario

Link		Elevation		L m	Diameter, mm		Thick. δ, mm
from	to	from	to		ND	ID	
R	J01	760	730	600	500	514.0	9.0
J01	P01	730	730	800	125	132.0	6.0
J01	J02	730	725	200	500	514.0	9.0
J02	P02	725	725	800	125	132.0	6.0
J02	J03	725	720	200	500	514.0	9.0
J03	P03	720	720	800	125	132.0	6.0
J03	J04	720	715	200	500	514.0	9.0
J04	P04	715	715	800	125	132.0	6.0
J04	J05	715	710	200	500	514.0	9.0
J05	P05	710	710	800	125	132.0	6.0
J05	J06	710	705	200	450	462.8	8.6
J06	P06	705	705	800	125	132.0	6.0
J06	J07	705	700	200	450	462.8	8.6
J07	P07	700	700	800	125	132.0	6.0
J07	J08	700	695	200	450	462.8	8.6
J08	P08	695	695	800	125	132.0	6.0
J08	J09	695	690	200	450	462.8	8.6
J09	P09	690	690	800	125	132.0	6.0
J09	T-2	690	680	400	350	362.6	7.7
J09	J10	690	685	200	250	260.4	6.8
J10	P10	685	685	800	125	132.0	6.0
J10	J11	685	680	200	200	209.4	6.3
J11	P11	680	680	800	125	132.0	6.0
J11	J12	680	675	200	200	209.4	6.3
J12	P12	675	675	800	125	132.0	6.0
J12	J13	675	670	200	150	158.0	6.0
J13	P13	670	670	800	125	132.0	6.0

## RESULTS AND VERIFICATION OF MATHEMATICAL MODEL

The verification of the results of the mathematical model HTM is made with the commercial software for analysis of the water hammer in complex systems HAMMER [3]. In addition to these images are the results obtained from the developed mathematical model HTM and the results obtained from the software package HAMMER.



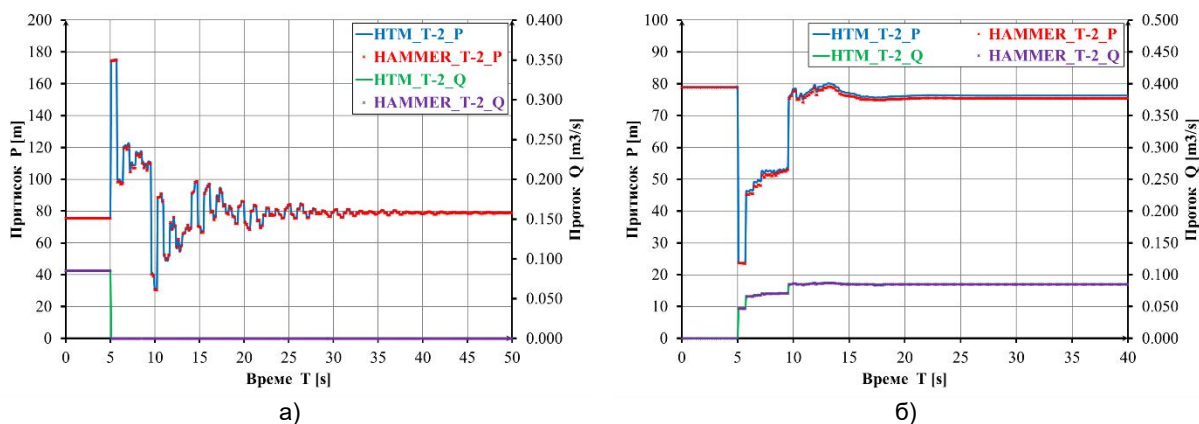


Figure 5. Results when abrupt closing (a) and opening (b) of the valve in the junction T-2

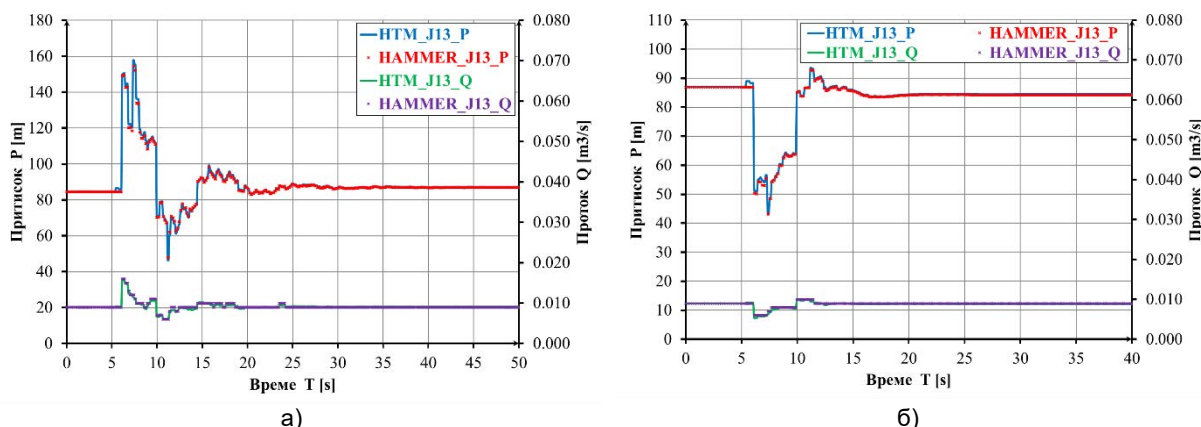


Figure 6. Results when abrupt closing (a) and opening (b) of the valve in the junction J13

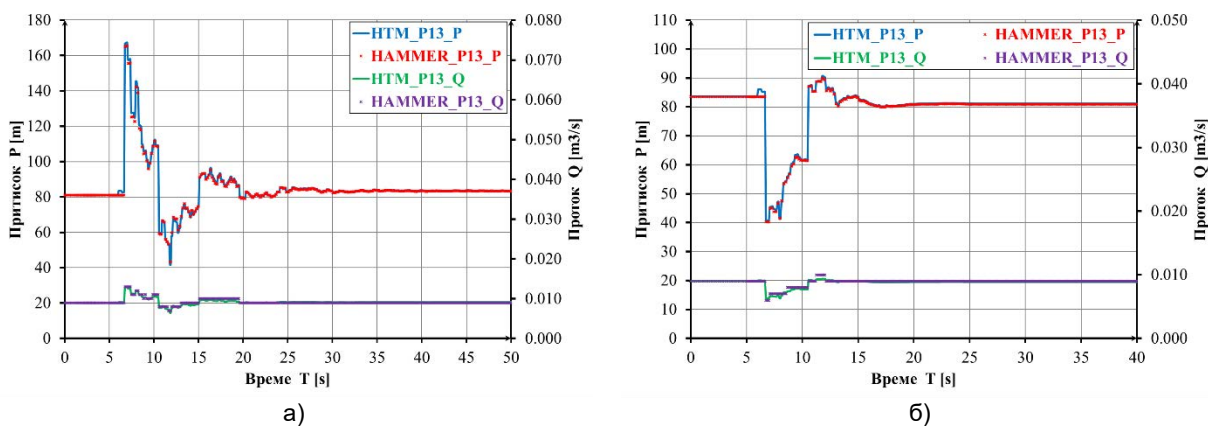


Figure 7. Results when abrupt closing (a) and opening (b) of the valve in the junction P13

## CONCLUSION

The algorithm of the mathematical model HTM is developed using the Visual Basic application in Excel whereby a "pleasant" program is procured to analyze the water hammer in the water supply systems. However, because it is a mathematical model that analyzes complex systems with extensive mathematical operations it is preferably before using the mathematical model the same to be subject to output results - verification of the model.

From the previously presented results, it can be concluded that the results of the mathematical model HTM near the initiator of unsteadiness completely overlaps with the results obtained from the software package HAMMER. By increasing the distance of the analyzed point of the initiator of the unsteadiness appear certain discrepancies in the results of the mathematical model HTM in terms of the software HAMMER. However, it may be noted that these deviations are very small, i.e. the deviations in the results are with the magnitude less than 5%. With such a small

value in deviations of the results in such complex systems it is deemed that the mathematical model HTM matches the results of the already existing software as HAMMER.

This overlapping of the results shows that the mathematical model HTM and the software package HAMMER use the same methods for solving complex equations that describe the phenomenon of water hammer i.e. both software's use method of characteristics as the most appropriate method for programming. It can also be concluded that the equations of characteristics for determining the boundary conditions are identical.

According to the previous one can conclude that the developed mathematical model HTM can be applied to analyze the water hammer in the water networks and that it gives results with sufficient accuracy of the change of pressure and flow throughout the entire water system.

## REFERENCES

- [1] Goce Taseski: „Characteristics of water hammers in water supply networks“. Doctorate dissertation, Skopje, Macedonia, 2015
- [2] Cvetanka Poposka: „Hydraulics“. Publisher Civil Engineering Faculty, University Ss. Cyril and Methodius, ISBN 9989-43-100-0, 2000.
- [3] Zhivko Veljanovski „Water supply“, Publisher Civil Engineering Faculty, University Ss. Cyril and Methodius, ISBN 978-9989-2922-1-7, 2008.
- [4] Bentley HAMMER V8i Edition User's Guide.
- [5] Streeter, V. L., Wylie, E.B., Hydraulic Transient, McGraw Hill Book Company, New York. 1967.
- [6] A.R.D. Thorley: Fluid Transients in Pipeline Systems, Second Edition (Pipelines and Pressure Vessels), Publisher: The American Society of Mechanical Engineers; 2nd edition, ISBN-13: 978-0791802106, 2004.
- [7] Kaveh Hariri Asli: “Water Hammer Research: Advances in Nonlinear Dynamics Modeling”, Publisher: Apple Academic Press, ISBN 9781926895314 - CAT# N10708, 2013.
- [8] A, Betamino de Almeida, E: “Fluid transient in Pipe Networks”, Publisher: WIT Press, ISBN-13: 978-1853121678, 1992.
- [9] Josef Zaruba: “Water hammer in pipe-line systems”, Publisher: Elsevier Science, ISBN-13: 978-0444987228, 1993.
- [10] John Parmakian: “Water hammer Analysis”, Publisher: Prentice Hall, Inc.; 1st edition, ASIN: B0000CJ5U0, 1995.
- [11] Fox, J.A. “Hydraulic analysis of unsteady flow in pipe networks”. Publisher: Macmillan Press Ltd, London, UK, ISBN-13: 978-0470270370. 1977.
- [12] Izquierdo, J., Inglesias, L.P., “Mathematical modelling of hydraulic transients in complex systems”. Mathematical and Computer Modelling, 39,529-540, 2004.
- [13] Simulation of Water Hammer Flows with Unsteady Friction Factor, ARPN Journal of Engineering and Applied Sciences, 2006.
- [14] Thomas Repp, Fluid Dynamic Water Hammer Simulations with Consideration of Fluid-Structure Interaction, <https://www.hzdr.de/FWS/publikat/JB98/jb08.pdf>, 2011.
- [15] A.R. Lohrasbi, R. Attarnejad “Water Hammer Analysis by Characteristic Method” American J. of Engineering and Applied Sciences 1 (4): 287-294, 2008.
- [16] Roman Wichowski, Hyd Archives of Hydro-Engineering and Environmental Mechanics Vol. 53 (2006), No. 3, pp. 267–291 Hydraulic Transients Analysis in Pipe Networks by the Method of Characteristics (MOC).

## DETERMINATION OF THE COEFFICIENT $\psi_2$ TO DEFINE LONG-TERM EFFECTS ON CONCRETE ELEMENTS UNDER VARIABLE LOAD

### AUTHORS

#### **Darko Nakov**

Ph.D. Assistant Professor  
Ss. Cyril and Methodius University  
Faculty of Civil Engineering – Skopje  
[nakov@gf.ukim.edu.mk](mailto:nakov@gf.ukim.edu.mk)

#### **Goran Markovski**

Ph.D. Professor  
Ss. Cyril and Methodius University  
Faculty of Civil Engineering – Skopje  
[markovski@gf.ukim.edu.mk](mailto:markovski@gf.ukim.edu.mk)

#### **Toni Arangelovski**

Ph.D. Assistant Professor  
Ss. Cyril and Methodius University  
Faculty of Civil Engineering – Skopje  
[arangelovskitoni@gf.ukim.edu.mk](mailto:arangelovskitoni@gf.ukim.edu.mk)

#### **Peter Mark**

Ph.D. Professor  
Ruhr-University Bochum, Germany  
Institute of Concrete Structures  
[massivbau@rub.de](mailto:massivbau@rub.de)

During the past 12 years, research project regarding time-dependent behavior of concrete elements is ongoing continuously at the Faculty of Civil engineering in Skopje. Experiments were performed on different types of concrete: prestressed, normal and high strength and steel fibre reinforced concrete, with various loading histories. The time-dependent changes in strains, deflections and crack widths were observed in a period of 400 days. This paper presents the effects of variable load on time-dependent behaviour of different types of concrete elements and proposes methodology for determination of coefficient  $\psi_2$ .

**Keywords:** quasi-permanent coefficient  $\psi_2$ , variable load, shrinkage, creep, Model B3

### INTRODUCTION

Long-term actions cause significant changes in concrete and reinforcement strain, increase in crack width and deflections, reduction of the tension stiffening and increase in bond-slip[3].

Besides this, degradation of concrete structures is usually medium to long-term process that has great influence on structure's working life. Among specific common causes responsible for structural degradation, action of variable loads is especially important issue for the assessment of long-term effects due to creep and shrinkage in concrete structures.

The effect of long-term actions is usually connected with the permanent load. However, there are certain concrete structures such as: storage areas at warehouses, traffic areas at parking garages and bridges under severe traffic conditions, where the variable loads are acting longer and are with significant magnitude. In these structures, the variable actions could overcome serviceability limit state criteria of concrete structure.

Because of previously stated reasons, in Eurocodes [6] in the serviceability limit design, assessment of effects due to creep and shrinkage of concrete caused by variable load are taken into consideration using quasi-



permanent combination of actions (also used for reversible limit states). The level of quasi-permanent load is defined by the quasi-permanent coefficient  $\psi_2$  (Eq.1):

$$\sum_{j \geq 1} G_{k,j} + "P" + \psi_{2,1} \cdot Q_{k,1} + \sum_{j \geq 1} \psi_{2,i} \cdot Q_{k,i} \quad (1)$$

The values for the quasi-permanent coefficient  $\psi_2$  could be set also by the National Annex. This gives opportunity for research of effects of variable load and its replacement by a quasi-permanent load by the coefficient of participation  $\psi_2$ .

In EN 1990: Eurocode - Basis of structural design [5], proposed values for the quasi-permanent coefficient for buildings are presented in Tab.1.

The recommended values for  $\psi_2$  for road bridges in EN 1990 is 0 [5]. In DIN report 102 "Concrete bridges" based on Eurocodes, for city bridges  $\psi_2$  is assumed to 0.2 and in the National application document of Finland for EN 1992-2,  $\psi_2=0.3$ . The recommended value of  $\psi_2$  factor for railway bridges is equal to zero. But if deformation is considered for persistent and transient design situations,  $\psi_2$  should be taken equal to 1.00 for rail traffic actions (according to Table A2.3 of EN1990:2002 [5]).

**Table 1.** Recommended values of coefficient  $\psi_2$  for buildings [5]

Action	$\psi_2$
Imposed loads in buildings, category (see EN1991-1-1)	
Category A: domestic, residential areas	0.3
Category B: office areas	0.3
Category C: congregation areas	0.6
Category D: shopping areas	0.6
Category E: storage areas	0.8
Category F: traffic area, vehicle weight $\leq 30\text{kN}$	0.6
Category G: traffic area, $30\text{kN} < \text{vehicle weight} \leq 160\text{kN}$	0.3
Category H: roofs	0.0

### METHODOLOGY FOR DETERMINATION OF THE COEFFICIENT $\psi_2$

This proposal in Eurocode was the basis of the extensive experimental and theoretical research, for determination of the quasi-permanent coefficient  $\psi_2$ .

Four approaches for determination of the effects of variable long-term actions were considered (Fig.1):

1. from point of zero value of deflection to obtain the value of experimentally determined deflection at the level of action of the permanent load.
2. from point of zero value of deflection to obtain the value of experimentally determined deflection at the level of action of the permanent and variable load.
3. from point of instantaneous value of deflection at permanent load level, (obtained at the first cycle of loading/unloading by variable load) to obtain the value of experimentally determined deflection at action of the permanent load.
4. from point of instantaneous value of deflection at permanent load level, (obtained at the first cycle of loading/unloading by variable load), to obtain the value of experimentally determined deflection at action of the permanent and variable load.

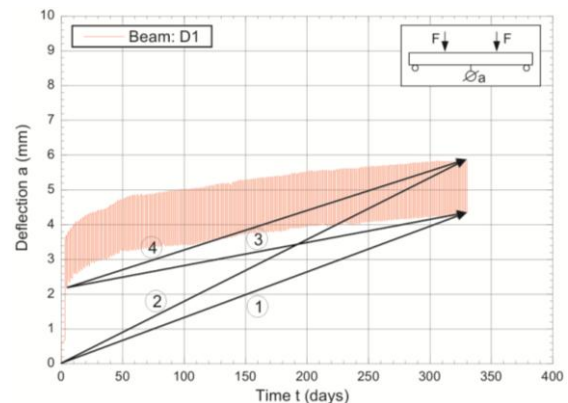


**Figure 1.** Considered approaches for determination of  $\psi_2$

The simplest solution of the problem is taking into consideration the approach 1, because with intensity of the load as sum of permanent and quasi-permanent load, we can obtain initial and time-dependent deflection.

On the basis of experimental research, analytical solution was proposed in which the total deflection from permanent load  $G$  and variable load  $Q$  obtained from the experiments at,  $exp(G+Q)$  is determined as a sum of the initial deflection  $a_0(G+\psi_2Q)$  and long-term deflection at  $(G+\psi_2Q)$  from permanent load  $G$  and variable load represent as quasi permanent load  $\psi_2Q$  (Eq.2):

$$a_{t,exp}(G+Q) = a_0(G + \psi_2 Q) + a_t(G + \psi_2 Q) \quad (2)$$

## EXPERIMENTAL PROGRAM

The research project consists of 3 experimental programs, denoted as follows:

- Experimental program "PC" (Prestressed concrete) [8];
- Experimental program "HSC" (High strength concrete) [1];
- Experimental program "SFRC" (Steel fiber reinforced concrete) [9].

The experiments were performed in specially equipped laboratory, located at the Faculty of Civil Engineering – Skopje. The laboratory (Figure 2) enables almost constant temperature, while the relative humidity is controlled with special humidifiers/dehumidifiers to keep it constant.



Figure 2. Part of the laboratory for testing

Each of the experimental programs consists of 24 full scale beams and control specimens for testing of the mechanical and deformation properties of concrete. The beams are with cross section  $b/d=15/28\text{cm}$  and length of 300cm. The geometry, inbuilt reinforcement and loading scheme for each experimental program is presented in Figure 3.

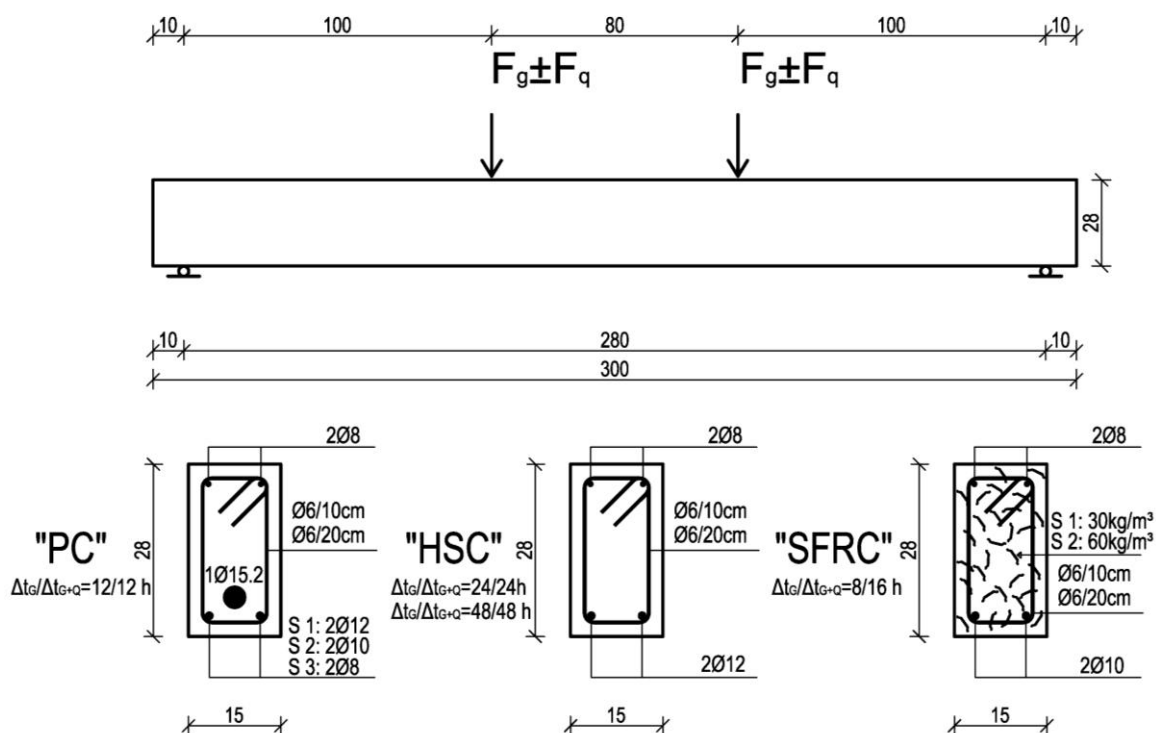
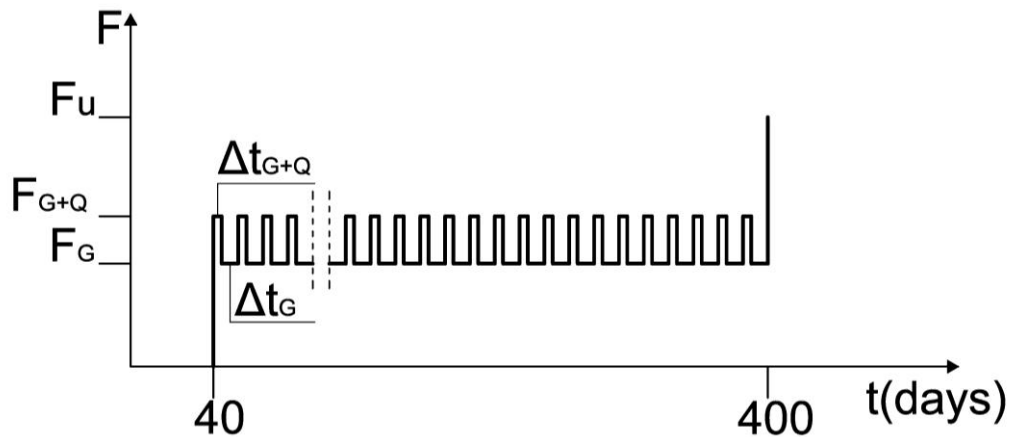


Figure 3. Geometry, reinforcement and loading scheme of the beams

Table 2. Cycles of the loading histories

cycles	Experimental program			
	PC	HSC	SFRC	
$\Delta t_G$ (hours)	12	24	48	8
$\Delta t_{G+Q}$ (hours)	12	24	48	16



**Figure 4.** Loading history of the beams

The beams were loaded at the age of 40 days with the specific loading history and at the age of 400 days the beams were loaded to failure. Loading histories were defined by action of constant permanent load and variable load acting in different cycles of loading/unloading, presented in Table 2 and in Fig.4.

## RESULTS

For each of the research projects, the following mechanical properties of concrete were tested at the same age as the testing of the full scale beams: Modulus of elasticity, compressive strength, splitting tensile strength and flexural tensile strength. Creep and drying shrinkage, as well as autogenous shrinkage in the case of the high-strength concrete were measured for 400 days continuously.

The testing of the mechanical and deformation properties is presented in Fig.5. The testing was performed at the age of 40 days and at the age of 400 days.

The experimental results of deformation properties of the research project "HSC" are presented in Fig.6.

For analytical analysis, evaluation of the autogenous shrinkage, drying shrinkage and creep strains (Fig.7a) was performed by using the B3 Model (Bazant & Baweja 2000) [2]. This analysis provide data to define improved B3 model compliance function  $J(t,t')$ , aging coefficient  $\chi(t,t')$  and relaxation function  $R(t,t')$ . All these parameters were used to calculate and to verify long-term deflections by age adjusted effective modulus method (AAEMM method) [4].

In the "SFRC" part of the research project, which analytical analysis are still undergoing, B3 Model [2] and fib Model code 2010 [7] are used to obtain the necessary data for the AAEMM. This will be done not only for the period of observing the full scale beams of approximately 1 year, but for an age of up to 100 years which is the life design age for certain structures. The analysis of the creep strain after 100 years in logarithmic scale is presented in Fig.7b.

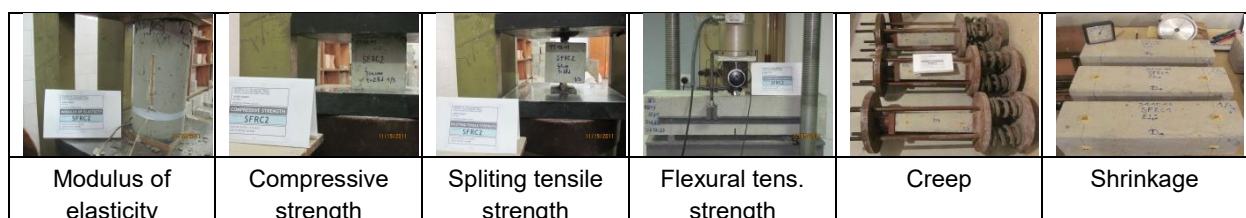


**Figure 5.** Testing of the mechanical and deformation properties



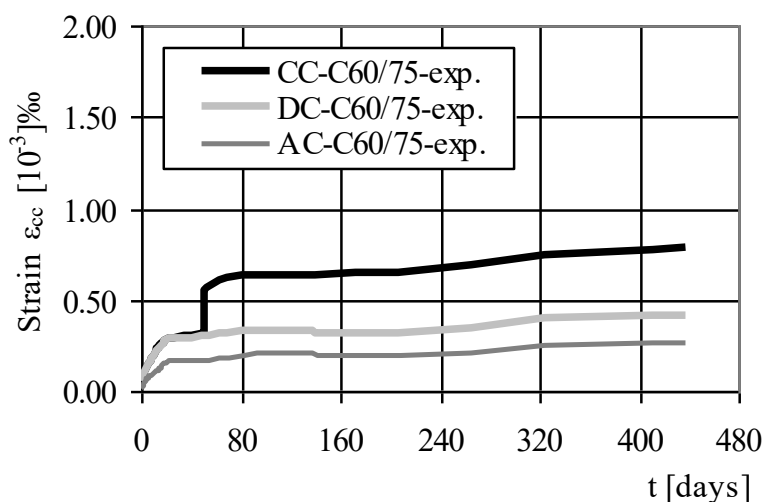


**Figure 6.** Total strain composed of autogenous shrinkage, drying shrinkage and creep in “HSC”

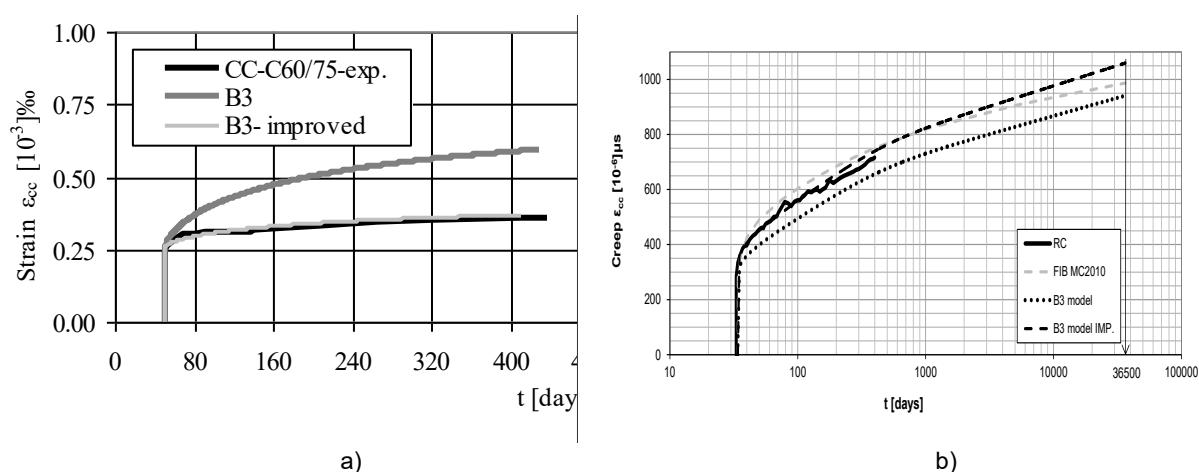


**Figure 7.** a) Analysis of the creep strain by the B3 model in “HSC” [1]; b) Analysis of the creep strain by B3 Model and fib MC2010 in “SFRC” [9]

In the “PC” part of the research project, modeling and analysis of the behaviour of prestressed concrete beams exposed to different history of loading during time were performed with the computer software program SOFISTIK using the finite element method.

To calculate effects from variable action on long-term deflections of concrete elements quasi-permanent load procedure and the

principle of superposition were used. The analysis of the long-term deflection for the experimental program “HSC” is presented in Fig.8a, while for the experimental program “PC” is presented in Fig.8b.

Obtained quasi-permanent coefficients  $\psi_2$  for each experimental program of the research project, for the considered time period of 400 days, are presented in Tab.3.

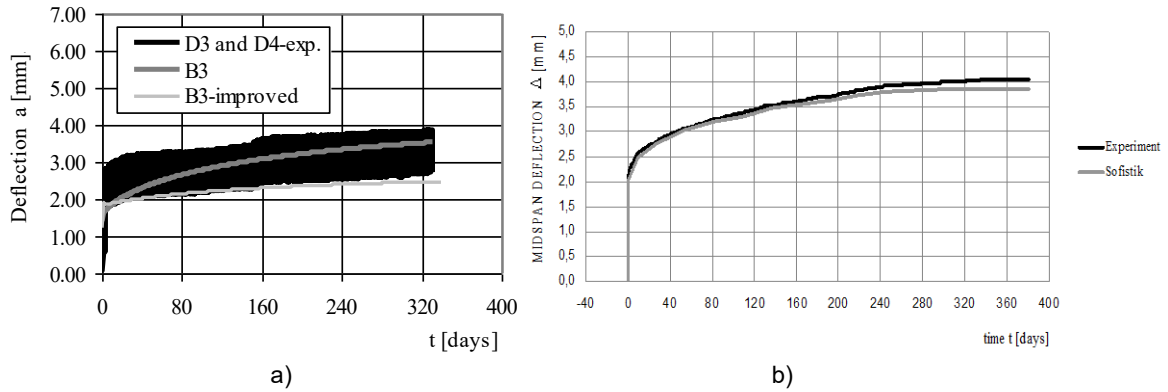


Figure 8. Analysis of the long-term deflection in experimental program: a) "HSC" [1] b) "PC" [8]

Table 3. Quasi-permanent coefficient  $\psi_2$  for each experimental program for time period of 400 days

cycles	Experimental program			
	PC	HSC		SFRC
$\Delta t_G$ (hours)	12	24	48	8
$\Delta t_{G+Q}$ (hours)	12	24	48	16
		$\psi_2$		
Ordinary concrete	/	0.50	0.65	0.37
PC /HSC /SFRC	0.40	1*	1*	0.20

\*Not realistic. Comes out from the low stress level.

A simple linear dependence between factor  $\psi_2$  and the variable load duration was found out and is presented in the following Fig.9. From

the same figure, almost double decrease of the factor  $\psi_2$  can be noticed, when steel fibres are added to the concrete mixture.

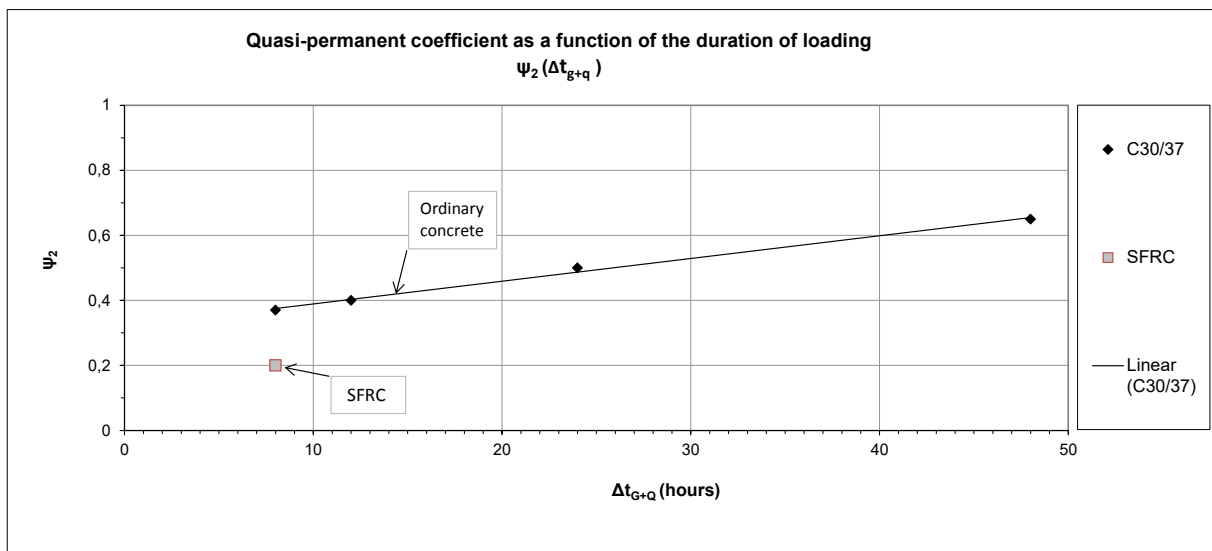


Figure 9. Factor  $\psi_2$  as a function of the variable load duration ( $\Delta t_{G+Q}$ )

## CONCLUSION

From the experimental and analytical analyses of the long-term behavior of beams made of different types of concrete, subjected to long-term permanent and variable load, the following conclusions can be drawn:

- Actions of long-term permanent and variable load have significant influence on the long-term behavior of concrete beams.
- The quasi-permanent coefficient  $\psi_2$  depends on the loading history, i.e. especially on the duration of the cycles when the variable load is acting on the structure ( $\Delta tG+Q$ ).
- For determination of the value of the quasi-permanent coefficient  $\psi_2$ , the stress and strain states of the cross sections for the different combinations of load cases should be taken into account.

## REFERENCES

- [1] Arangelovski, T.: Time-dependent behavior of reinforced high-strength concrete elements under action of variable loads, Doctoral dissertation, Skopje: University "Ss. Cyril and Methodius", 2010.
- [2] Bazant Z.P. & and Baweja, S.: Creep and Shrinkage Prediction Model for Analysis and Design of Concrete Structures: Model B3, The Adam Neville Symposium: Creep and Shrinkage-Structural Design Effects, SP-194, American Concrete Institute 2000, Akthem Al-Manaseer (ed.), Farmington Hills: ACI, 2000.
- [3] CEB Bulletin d'information No 235.: Serviceability Models-Behaviour and modelling in serviceability limit states including repeated and sustained loads. G. Balazs (eds). Lausanne, 1997.
- [4] Jirasek, M. & Z.P.Bazant.: Inelastic Analyses of Structures, London: John Wiley & Sons, 2001.
- [5] European Standard EN1990.: Basis of structural design, Standardization Institute of R.Macedonia, Skopje, R.Macedonia, 2002.
- [6] European Standard EN1992-1-1.: Eurocode 2: Design of concrete structures - Part 1-1: General rules and rules for buildings, Standardization Institute of R.Macedonia, Skopje, R.Macedonia, 2004.
- [7] Fib Model Code 2010.: fib Bulletin 65, Final draft, 2012.
- [8] Markovski, G.: Influence of variable loads to time-dependant behavior of prestressed concrete elements, Doctoral dissertation, Skopje: University "Ss. Cyril and Methodius", 2003.
- [9] Nakov, D.: Time-dependent behaviour of SFRC elements under sustained and repeated variable loads, Doctoral dissertation, Skopje: University "Ss. Cyril and Methodius", 2014.



*We restore the past...*  
*We build the future...*



**TRAN**Sport • **M**ining • **E**ngineering • **T**rading

Address: Str. Kosturski heroj No. 38, floor 2, local 1, 1000 Skopje  
tel: +389 2 2720 411; +389 2 2775 311 || fax: +389 2 2720 411  
e-mail: [info@transmet.com.mk](mailto:info@transmet.com.mk) || [www.transmet.com.mk](http://www.transmet.com.mk)

## CONTRIBUTION TO THE ANALYSIS OF REINFORCED BEAMS - PART I

### AUTHOR

**Dr. Ing. Mile R. MIHAJLOV**

Former Assistant

Ss. Cyril and Methodius University, Macedonia

Faculty of Civil Engineering, Skopje

[milemihajlov@yahoo.com](mailto:milemihajlov@yahoo.com)

In this paper is presented theoretical analysis for estimating internal stresses in reinforced beams. A basic beam is reinforced with thin lamella which is glued to one side of the beam. The beam ends are loaded with pure bending couple, thus inducing only bending stresses in the beam. But, on the other hand, the lamella on the top of the beam is subjected to tensile stresses as well as bending stresses. The object of this paper is deriving expressions for calculating the internal stresses. For the theoretical analysis, the principal of minimum complimentary strain energy is applied [6,7] Thus the principal of virtual internal self equilibrating stresses is used. The contributions in this paper are that theoretical expressions are derived for the forementioned objects.

The knowledge of direct and shear stresses in the glue layer are no longer unknown.

This allows proper design of such lamella reinforcement for beams, subjected to bending moments. The theoretical derivations apply to all combinations of materials. They can be wood to wood, metal to metal, metal to plastics (FRP), wood to metal, and other combinations. The formulas derived are quite general for use.

**Keywords:** shear stress, direct stress, glue layer, top lamella, main beam, equilibrium.

### INTRODUCTION

In the engineering practice reinforced beams play an important role. They are common to civil engineering, aeronautical engineering and mechanical engineering. There is no structure in the forementioned branches, that is not making use of them. The reinforced beams are performed nowadays with bolts, rivets, nails, welding, and gluing with epoxy resin. They have good and weak properties. For example, the riveted joints have the disadvantage of becoming looser with time, under dynamic loading. Also, together with the bolted connection they reduce the effective area of the element due to the holes. Thus making the joint less efficient in direct tensile load. Not only that, but the holes induce stress-concentration and reduce the life of the connection under dynamic loading. But all

these disadvantages are overcome by careful theoretical considerations in their analysis.

More recently, new technology reinforced beams [1] have been introduced in engineering practice, particularly in civil engineering. They are the glued reinforced beams with epoxy resin. For their reliable use, theoretical analysis is required for the stresses in the basic material and the glue. Also aluminium beams reinforced with steel lamella are common to engineering.

In this paper the main concern are the internal stresses in the reinforced beam, subjected to pure bending moment.

## THEORETICAL ANALYSIS

In this paper we are concerned with the estimate of internal stresses in reinforced beam subjected to external loading. The structure to be analyzed is shown in fig. 1.

It consists of main beam of given dimensions and material, and top lamella that is glued on to the beam. The dimensions of the lamella are different from those of the main beam and is made from same or different material.

The main beam is subjected to pure bending couple at its ends which is inducing bending direct and shear stresses. As a consequence of deformations of the connection, tensile and shear loads are induced in the top lamella together with the glue layer.

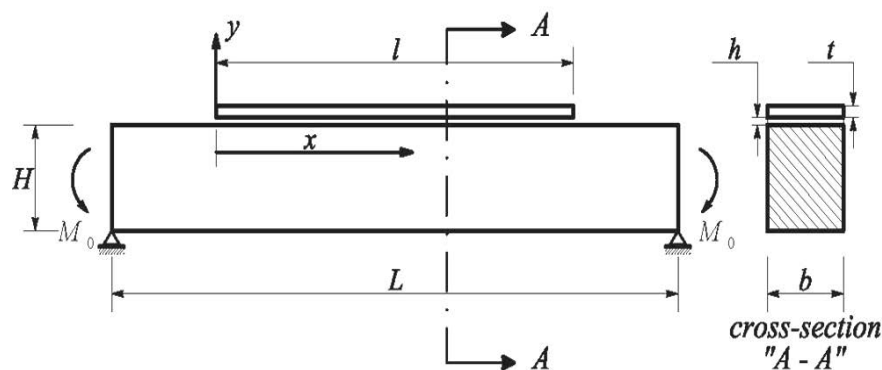


Figure 1. Lay out of the reinforced beam to be analyzed.

Basic assumption is made that cross-sections into the region of connection between the beam and lamella, which are straight before deformation, remain straight lines-planes after the deformation of the reinforced beam. So that for distribution of direct strains Bernoulli hypothesis of straight planes apply. But due to the shear strains that are no longer small quantities, warping of the cross-section takes place. As far as the glue layer is concerned the following can be said. The shear stresses in the glue are also large quantities. They are of significant values towards the ends of the top lamella. As a consequence of these shear stresses, direct, normal to the glue layer, stress takes place at the end of the glue layer. But, the longitudinal axial stress in the glue layer can be neglected in comparison to the tensile and compressive stresses in the top lamella and basic beam. This follows from the fact that longitudinal strains in the glue are of same order as the longitudinal strains in the lamella and beam. But the modulus of

elasticity of the glue is much smaller than those of the top lamella and the beam.

As mentioned before, we shall use the principle of minimum complementary strain energy, i.e. the principle of virtual internal stresses to derive the generalized compatibility equations. For this to be done, we need to derive expressions for the internal stresses as a function of the reinforced beam dimensions and internal forces that take place. After that, the internal forces will be related to the externally applied bending moment, using the equilibrium equations.

As internal forces, we choose the tension  $T$  in the top lamella and the bending moment  $M$ , the tension  $T_1$  and the bending moment  $M_1$ , as internal forces of the main beam. The tensile load in the glue layer will be taken as zero, i.e. neglected, due to the reasons explained earlier. We shall begin the derivations by analyzing firstly the top element.



Let us consider the equilibrium equation for the plane stress [6] which is:

$$\frac{\partial \sigma_x}{\partial x} + \frac{\partial \tau}{\partial y} = 0 \quad (1)$$

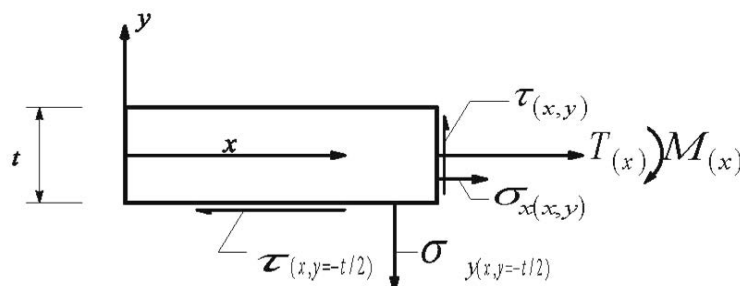


**Figure 2.** Part of the top lamella with indicated internal stresses and forces.

From the theory of strength of materials we can write that  $\sigma_x$  is given by the relation:

$$\sigma_x = \frac{T}{A} + \frac{y}{J} M; A = bt; J = \frac{bt^3}{12} \quad (2)$$

Differentiating w.r. to  $x$  the above expression and substitute in (1) yields:

$$\frac{\partial \tau}{\partial y} = -\frac{1}{A} \frac{dT}{dx} - \frac{y}{J} \frac{dM}{dx}$$

Integrating the above expression with respect to  $y$ , we obtain:

$$\tau = -\frac{y}{A} \frac{dT}{dx} - \frac{y^2}{2J} \frac{dM}{dx} + f_{(x)} \quad (3)$$

The function  $f_{(x)}$  will be determined from the boundary condition that:

$$\tau_{(y=t/2)} = 0$$

as a free surface. Hence, from relation (3), by substituting for  $y = t/2$  we get:

$$f_{(x)} = \frac{t}{2A} \frac{dT}{dx} + \frac{t^2}{8J} \frac{dM}{dx}$$

Finally, the formula for  $\tau$  is obtained in the form:

$$\tau = -\frac{1}{A} (y-t/2) \frac{dT}{dx} - \left( \frac{y^2}{2} - \frac{t^2}{8} \right) \frac{1}{J} \frac{dM}{dx} \quad (4)$$

The element considered is shown in fig. 2.

The above relation expresses the shear stress  $\tau$  as a function of the internal generalized forces  $T$  and  $M$  for top lamella.

Now we need to derive an expression for the  $\sigma_y$  direct stress in terms of  $T$  and  $M$  for the same element. To do this, use will be made of the second equilibrium equation for plane stress [6], i.e.

$$\frac{\partial \sigma_y}{\partial y} + \frac{\partial \tau}{\partial x} = 0 \quad (5)$$

For the above equation to be used, we need to obtain  $\partial \tau / \partial x$ . Differentiating equation (4) w.r. to  $x$  yields:

$$\frac{\partial \tau}{\partial x} = -\frac{1}{A} (y-t/2) \frac{d^2 T}{dx^2} - \left( \frac{y^2}{2} - \frac{t^2}{8} \right) \frac{1}{J} \frac{d^2 M}{dx^2}$$

Substituting the above relation into equation (5) and integrating with respect to  $y$ , we obtain:

$$\sigma_y = \frac{1}{A} \left( \frac{y^2}{2} - \frac{ty}{2} \right) \frac{d^2 T}{dx^2} + \left( \frac{y^3}{3} - \frac{t^2 y}{4} \right) \frac{1}{2J} \frac{d^2 M}{dx^2} + f_{I(x)} \quad (6)$$

The function of integration  $f_{I(x)}$  will be determined from the boundary condition that follows from a free surface:

$$\sigma_{y(y=t/2)} = 0$$

Using the above stated condition and inserted in equation (6), yields the following expression for  $f_{I(x)}$ :

$$f_{I(x)} = \frac{I}{A} \frac{t^2}{8} + \frac{d^2 T}{dx^2} + \frac{t^3}{24J} \frac{d^2 M}{dx^2} \quad (7)$$

Substituting the expression for  $f_{I(x)}$  from (7) into (6), we obtain:

$$\sigma_y = \frac{I}{A} \left( \frac{y^2}{2} - \frac{ty}{2} + \frac{t^2}{8} \right) \frac{d^2 T}{dx^2} + \left( \frac{y^3}{3} - \frac{t^2 y}{4} + \frac{t^3}{12} \right) \frac{1}{2J} \frac{d^2 M}{dx^2} \quad (8)$$

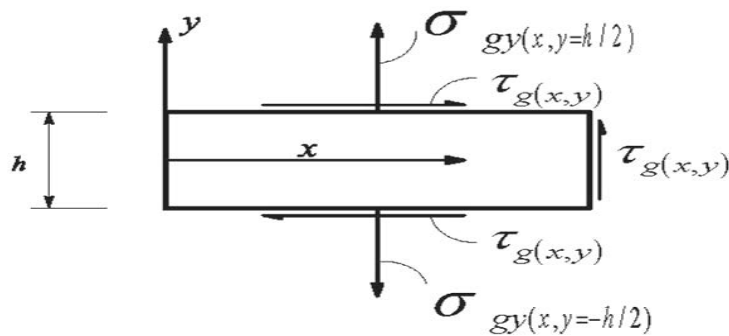


Figure 3. Part of the glue layer subjected to internal stresses.

The glue layer is subjected to shear stress  $\tau_g$  and direct stress  $\sigma_{yg}$ . The tensile stress  $\sigma_{xg}$  is neglected, due to explained reasons earlier.

The shear stress  $\tau_g$  must be same to that of the top lamella at the common surface. But it is assumed to be constant across the thickness of the layer, due to the assumption that  $\sigma_{xg} \cong 0$ . Therefore we can write that  $\tau_g$  is given by the expression:

$$\tau_g = \frac{1}{b} \frac{dT}{dx} \quad (9)$$

Having written the expression for  $\tau_g$ , the use of equation (5) leads to the determination of  $\sigma_{yg}$ . Thus, substituting for  $\tau_g$  from (9) into (5) yields:

$$\frac{\partial \sigma_{yg}}{\partial y} = -\frac{1}{b} \frac{d^2 T}{dx^2}$$

Integrating the above expression with respect to  $y$ , leads to the following expression for  $\sigma_{yg}$ :

The above formula is the required expression that relates  $\sigma_y$  direct stress to the internal generalized forces  $T$  and  $M$  for the top lamella.

Having derived the expressions for  $\tau$ ,  $\sigma_x$  and  $\sigma_y$  stresses for the top lamella, we turn on to derive the expressions for the internal stresses in the glue layer. Part of the glue layer to be analyzed is shown in fig. 3.

$$\sigma_{yg} = -\frac{1}{b} y \frac{d^2 T}{dx^2} + f_{2(x)} \quad (10)$$

The function of integration  $f_{2(x)}$  will be determined from the following boundary condition:

$$\sigma_{yg(y=h/2)} = \sigma_{yt(y=-t/2)}$$

Therefore from equations (8) and (10) follows that:

$$f_{2(x)} - \frac{h}{2b} \frac{d^2 T}{dx^2} = \frac{t}{2b} \frac{d^2 T}{dx^2} + \frac{1}{b} \frac{d^2 M}{dx^2}$$

Solving for  $f_{2(x)}$ , we obtain for  $f_{2(x)}$ :

$$f_{2(x)} = \frac{1}{2b} (t+h) \frac{d^2 T}{dx^2} + \frac{1}{b} \frac{d^2 M}{dx^2} \quad (11)$$

Substituting for  $f_{2(x)}$  from the above expression into equation (10), we obtain:

$$\sigma_{yg} = \frac{1}{b} \left( -y + \frac{t}{2} + \frac{h}{2} \right) \frac{d^2 T}{dx^2} + \frac{1}{b} \frac{d^2 M}{dx^2} \quad (12)$$

Formula (12) relates the direct stress  $\sigma_{yg}$  in the glue layer to the internal generalized forces  $T$  and  $M$  in the top lamella.

Before turning on deriving the stress-force relationship in the main beam, we shall derive the dependence between the internal forces in

the main beam  $T_1$  and  $M_1$  and the variables  $T$  and  $M$ .

For that purpose let us consider the equilibrium of generalized forces shown in fig. 4.

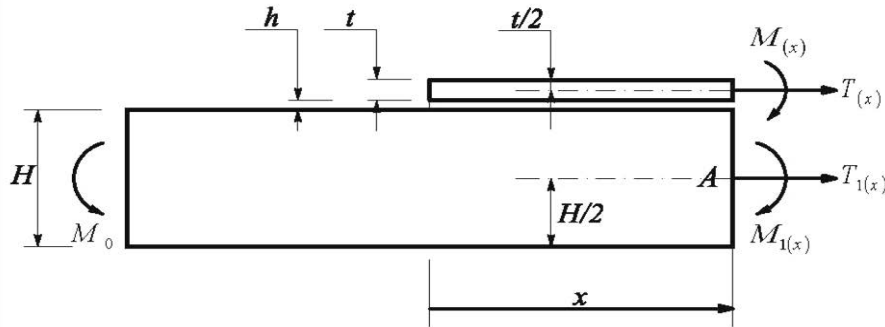


Figure 4. Free body diagram for internal and applied forces.

For horizontal equilibrium we can write that:

$$\Sigma F_x = 0 \quad T_1 + T = 0$$

therefore it follows that

$$T_1 = -T \quad (13)$$

for rotational equilibrium of moments, follows that

$$\Sigma M_A = 0 \quad M + M_1 + \frac{1}{2}(H+t)T - M_0 = 0$$

Hence, from the above equation, we can express  $M_1$  in terms of  $M$  and  $T$  via the relation:

$$M_1 = M_0 - M - \frac{1}{2}(H+t)T \quad (14)$$

Now remains to derive expressions for  $\sigma_{x1}$ ,  $\sigma_{y1}$  and  $\tau_1$  in terms of the generalized forces  $T$  and  $M$ . The direct stress  $\sigma_{x1}$  is given by the relation:

$$\sigma_{x1} = \frac{T_1}{A_1} + \frac{y}{J_1} M_1$$

Substituting for  $T_1$  and  $M_1$  from (13) and (14), yields the following formula for  $\sigma_{x1}$ :

$$\sigma_{x1} = -\frac{T}{A_1} - \frac{1}{2}(H+t)\frac{y}{J_1}T - \frac{y}{J_1}M + \frac{y}{J_1}M_0 \quad (15)$$

Having written the expression for the direct stress  $\sigma_{x1}$ , we continue deriving expression for the shear stress  $\tau_1$ . In the above relation (15)  $A_1$  is the cross-sectional area of main beam, and  $J_1$  is the second moment of area. To derive expression for  $\tau_1$ , similar to the derivation of  $\tau$  for the top lamella, we begin by making use of equation (1). Therefore we can write that:

$$\frac{\partial \tau_1}{\partial y} = \left[ \frac{1}{A_1} + \frac{1}{2}(H+t)\frac{y}{J_1} \right] \frac{dT}{dx} + \frac{y}{J_1} \frac{dM}{dx}$$

Integrating the above equation w.r. to  $y$ , one obtains:

$$\tau_1 = \left[ \frac{y}{A_1} + \frac{1}{4}(H+t)\frac{y^2}{J_1} \right] \frac{dT}{dx} + \frac{y^2}{2J_1} \frac{dM}{dx} + f_{3(x)} \quad (16)$$

The function of integration  $f_{3(x)}$  will be determined from the boundary condition:

$$\tau_{1(y=-H/2)} = 0$$

as a free surface. Hence, the following expression is obtained for the function  $f_{3(x)}$ :

$$f_{3(x)} = \left[ \frac{H}{2A_1} - \frac{1}{16}(H+t)\frac{H^2}{J_1} \right] \frac{dT}{dx} - \frac{H^2}{8J_1} \frac{dM}{dx} \quad (17)$$

Substituting back for  $f_{3(x)}$  from (17) into (16), final expression for the shear stress  $\tau_1$  is obtained in the form:

$$\tau_1 = \left[ \frac{1}{A_1} \left( y + \frac{H}{2} \right) + \frac{(H+t)}{4J_1} \left( y^2 - \frac{H^2}{4} \right) \right] \frac{dT}{dx} + \frac{1}{2J_1} \left( y^2 - \frac{H^2}{4} \right) \frac{dM}{dx} \quad (18)$$

Expression (18) relates the shear stress  $\tau_1$  in the main beam to the generalized forces  $T$  and  $M$ .

$$\frac{\partial \sigma_{y1}}{\partial y} = - \left[ \frac{1}{A_1} \left( y + \frac{H}{2} \right) + \frac{(H+t)}{4J_1} \left( y^2 - \frac{H^2}{4} \right) \right] \frac{d^2 T}{dx^2} - \frac{1}{2J_1} \left( y^2 - \frac{H^2}{4} \right) \frac{d^2 M}{dx^2}$$

Integrating the above expression with respect to  $y$ , we obtain the following relation for  $\sigma_{y1}$ :

$$\sigma_{y1} = - \left[ \frac{1}{A_1} \left( \frac{y^2}{2} + \frac{Hy}{2} \right) + \frac{(H+t)}{4J_1} \left( \frac{y^3}{3} - \frac{H^2 y}{4} \right) \right] \frac{d^2 T}{dx^2} - \frac{1}{2J_1} \left( \frac{y^3}{3} - \frac{H^2 y}{4} \right) \frac{d^2 M}{dx^2} + f_{4(x)} \quad (19)$$

The function of integration  $f_{4(x)}$  is determined from the boundary condition that  $\sigma_{y1}$  is zero at the free surface  $y = -H/2$ , i.e.

$$\sigma_{y1(y=-H/2)} = 0$$

Satisfying the above condition, the function  $f_{4(x)}$  gets the following value:

$$f_{4(x)} = - \left[ \frac{H^2}{8A_1} + \frac{(H+t)H^3}{48J_1} \right] \frac{d^2 T}{dx^2} + \frac{H^3}{24J_1} \frac{d^2 M}{dx^2} \quad (20)$$

Substituting the above value for  $f_{4(x)}$  into relation (19) yields the final expression for  $\sigma_{y1}$ :

$$\sigma_{y1} = - \left[ \frac{1}{A_1} \left( \frac{y^2}{2} + \frac{Hy}{2} + \frac{H^2}{8} \right) + \frac{(H+t)}{4J_1} \left( \frac{y^3}{3} - \frac{H^2 y}{4} - \frac{H^3}{12} \right) \right] \frac{d^2 T}{dx^2} - \frac{1}{2J_1} \left( \frac{y^3}{3} - \frac{H^2 y}{4} - \frac{H^3}{12} \right) \frac{d^2 M}{dx^2} \quad (21)$$

Formula (21) is the last required relationship for the further analysis of the reinforced beam. The previously derived expressions for the internal stresses in the top lamella, glue layer and the main beam will be used to derive the generalized compatibility equations. Before we begin deriving the generalized compatibility equations, explanation will be given on, for the application of the principal of minimum complimentary potential energy [6,7]. The principal of complimentary virtual work is:

$$\delta w^* = \delta U_d^* \quad (22)$$

In the above equation  $\delta w^*$  is the complimentary potential of external forces and  $\delta U_d^*$  is the internal virtual complimentary strain energy. Now, we choose the external virtual forces to be zero, and also choose the internal virtual stresses to be zero on the boundaries, then equation (22) reduces to:

$$\delta_\sigma U_d^* = 0$$

The index  $\sigma$  indicates that only virtual strains are varied. The above statement can be written in terms of strains and stresses as:

$$\int_V \{ \varepsilon_x \varepsilon_y \}^t \{ \delta \sigma_x \delta \sigma_y \} dV + \int_V \gamma \delta \alpha dV = 0 \quad (23)$$

In the relation (23)  $\varepsilon_x$ ,  $\varepsilon_y$  and  $\gamma$  represent real strains and  $\delta \sigma_x$ ,  $\delta \sigma_y$  and  $\delta \tau$  represent virtual complimentary internal stresses that are zero on the boundary of the structure.

We shall begin the derivation of the compatibility equation by evaluating the internal virtual complimentary strain energy of the glue layer. The virtual complimentary stresses for this part of the structure are:

$$\delta \tau_g = \frac{1}{b} \delta \left( \frac{dT}{dx} \right) \quad (24)$$



$$\delta\sigma_{yg} = \frac{1}{b} \left( \frac{t}{2} + \frac{h}{2} - y \right) \delta \left( \frac{d^2T}{dx^2} \right) + \frac{1}{b} \delta \left( \frac{d^2T}{dx^2} \right) \quad (25)$$

The internal virtual complimentary energy due to virtual complimentary shear stress is given by the expression:

$$\delta U_{g\tau}^* = \frac{1}{G_g} \int_0^l \int_{-h/2}^{h/2} \tau_g \delta\tau_g b dy dx \quad (26)$$

Substituting from (9) and (24) for  $\tau_g$  and  $\delta\tau_g$  into the above expression, yields:

$$\delta U_{g\tau}^* = \frac{1}{G_g b} \int_0^l \int_{-h/2}^{h/2} \frac{dT}{dx} \delta \left( \frac{dT}{dx} \right) dy dx$$

Evaluating the above integral by integration by parts, follows:

$$\delta U_{g\tau}^* = \frac{h}{G_g b} \left\{ \left[ \frac{dT}{dx} \delta T \right]_0^l - \int_0^l \frac{d^2T}{dx^2} \delta T dx \right\}$$

$$\delta U_{g\tau}^* = \frac{1}{E_g b} \int_0^l \int_{-h/2}^{h/2} \left[ \left( \frac{t}{2} + \frac{h}{2} - y \right) \frac{d^2T}{dx^2} + \frac{d^2M}{dx^2} \right] * \left[ \left( \frac{t}{2} + \frac{h}{2} - y \right) \delta \left( \frac{d^2T}{dx^2} \right) + \delta \left( \frac{d^2M}{dx^2} \right) \right] dy dx$$

Choosing the complimentary virtual generalized forces  $\delta T$  and  $\delta M$  and their derivatives  $\delta T'$  and  $\delta M'$  to be zero at  $x=0$  and

As mentioned earlier, we choose the virtual complimentary tensile load  $\delta T$  to be zero at  $x=0$  and  $x=l$ . Thus we obtain:

$$\delta U_{g\tau}^* = -\frac{1}{G_g b} \int_0^l \frac{d^2T}{dx^2} \delta T dx \quad (27)$$

The part of the internal virtual complimentary energy due to the virtual complimentary direct stress  $\sigma_{yg}$  is given by the expression:

$$\delta U_{\tau\sigma}^* = \frac{1}{E_g} \int_0^l \int_{-h/2}^{h/2} \sigma_{yg} \delta\sigma_{yg} b dy dx \quad (28)$$

Substituting from (12) and (25) for  $\sigma_{yg}$  and  $\delta\sigma_{yg}$  into expression (28) we get:

$x=l$ , as before, the above double integral becomes:

$$\delta U_{g\sigma}^* = \frac{1}{bE_g} \left\{ \left( \frac{4h^3 + 6th^2 + 3t^2h}{12} \right) \int_0^l \frac{d^4T}{dx^4} \delta T dx + \left( \frac{h^2th}{2} \right) \int_0^l \frac{d^2M}{dx^4} \delta T dx + \left( \frac{h^2 + th}{2} \right) \int_0^l \frac{d^4T}{dx^2} \delta M dx + h \int_0^l \frac{d^4M}{dx^4} \delta M dx \right\} \quad (29)$$

Hence, from expression (23), (27) and (29) the complimentary virtual strain energy in the glue layer is given by the sum:

$$\delta U_g^* = \delta U_{g\tau}^* + \delta U_{g\sigma}^*$$

In similar way, we can derive the expressions for the virtual complimentary strain energy in the top lamella and main beam. But due to long derivations [4,5] involving double integrals, they will not be given in this paper.

Hence the derived system of two differential equation of generalized compatibility will be stated in the form:

$$[k] \begin{Bmatrix} T^{IV} \\ M^{IV} \end{Bmatrix} + [B] \begin{Bmatrix} T^{II} \\ M^{II} \end{Bmatrix} + [C] \begin{Bmatrix} T \\ M \end{Bmatrix} = \{R\} \quad (30)$$

In the above matrix differential equation of generalized compatibility, the coefficient's matrices  $[k]$ ,  $[B]$  and  $[C]$  are given by the following matrix relations:

$$[k] = \frac{1}{E_g b} \begin{bmatrix} \left( \frac{4h^3 + 6th^2 + 3t^2h}{12} \right) & \left( \frac{h^2 + th}{2} \right) \\ \left( \frac{h^2 + th}{2} \right) & h \end{bmatrix} + \frac{1}{Eb} \begin{bmatrix} \frac{t^3}{20} & \frac{t^2 12}{90} \\ \frac{t^2 12}{90} & \frac{13t}{35} \end{bmatrix} + \frac{1}{E_1 b} \begin{bmatrix} \left( \frac{4H^3 + 22H^2t + 39t^2H}{420} \right) & \left( \frac{11H^2 + 39tH}{210} \right) \\ \left( \frac{11H^2 + 39tH}{210} \right) & \frac{13H}{35} \end{bmatrix} \quad (31a)$$

$$[B] = - \begin{bmatrix} \frac{h}{G_g b} & 0 \\ 0 & 0 \end{bmatrix} - \frac{1}{G_1 b} \begin{bmatrix} \left( \frac{4H^2 + 3tH^2 + 9t^2}{30H} \right) & \left( \frac{H + 6t}{10H} \right) \\ \left( \frac{H + 6t}{10H} \right) & \frac{6}{5H} \end{bmatrix} - \frac{1}{b} \begin{bmatrix} \frac{t \left( \frac{\nu}{E} + \frac{1}{G} \right)}{3} & \frac{1}{2G} \\ \frac{1}{2G} & \frac{6 \left( \frac{1}{G} - \frac{2\nu}{E} \right)}{5t} \end{bmatrix} + \frac{\nu_1}{bE_1} \begin{bmatrix} \left( \frac{4H^2 + 18tH + 9t^2}{15H} \right) & \frac{12 \left( \frac{H+t}{H} \right)}{10} \\ \frac{12 \left( \frac{H+t}{H} \right)}{10} & \frac{12}{5} \frac{1}{H} \end{bmatrix} \quad (31b)$$

$$[C] = \frac{1}{bE_1} \begin{bmatrix} \left( \frac{4H^2 + 6tH + 3t^2}{H^3} \right) & \frac{6(H+t)}{H^3} \\ \frac{6(H+t)}{H^3} & \frac{12}{H^3} \end{bmatrix} + \frac{1}{bE} \begin{bmatrix} \frac{1}{t} & 0 \\ 0 & \frac{12}{t^3} \end{bmatrix} \quad (31c)$$

The no homogeneous term  $\{R\}$  is given by the matrix expression:

$$\{R\} = \begin{Bmatrix} \frac{6(H+t)}{H^3} \\ \frac{12}{H^3} \\ \frac{6(H+t)}{H^3} \end{Bmatrix} \frac{M_0}{bE_1} \quad (32)$$

The matrix equation (30) can be solved in several ways. We shall do it in standard way by obtaining the complementary solution and particular integral. The complementary solution is foreseen in the form:

$$\begin{Bmatrix} T \\ M \end{Bmatrix} = \begin{Bmatrix} y_1 \\ y_2 \end{Bmatrix} e^{\lambda x} = \{y\} e^{\lambda x} \quad (33)$$

Substituting the assumed solution (33) into (30) yields:

$$\lambda^4 [k] \{y\} + \lambda^2 [B] \{y\} + [C] \{y\} = \{0\} \quad (34)$$

Introducing the substitution:

$$\beta = \lambda^2$$

and substituting into matrix equation (34), yields the following matrix relation:

$$\beta^2 [k] \{y\} + \beta [B] \{y\} + [C] \{y\} = \{0\} \quad (35)$$

The matrix equation (35) represents standard damped eigen value problem, whose solution [2] can be obtained by standard numerical methods.

The nature of solution for the eigen values  $\lambda_i$  and eigen vectors  $\{y\}_i$  strongly depends on the elastic constants of the materials used, and the dimensions of the reinforced beam. They can be real, complex and pure imaginary. In case some of them are pure imaginary, no solution exists for the analysis of the reinforced beam. If they are all real, or mixed real and complex eigen values, the solution exists. The form of the solution will be demonstrated on a particular example given in this paper.

As far as the particular solution is concern, since the vector  $\{R\}$  is constant, not function of  $x$ , the particular integral is given by the matrix equation:

$$\begin{Bmatrix} T \\ M \end{Bmatrix}_p = [C]^{-1} \{R\} \quad (36)$$

The complete solution will be given by the sum of the complimentary solution and the particular integral, i.e.

$$\begin{Bmatrix} T \\ M \end{Bmatrix} = \sum_{i=1}^{i=4} A_i \begin{Bmatrix} y_1 \\ y_2 \end{Bmatrix}_i e^{\lambda_i x} + \begin{Bmatrix} T \\ M \end{Bmatrix}_\rho \quad (37)$$

In the above solution four constants  $A_i$  of integration take place. They will be determined from the following boundary conditions.

At the cross-section  $x=0$ , as a free edge,  $T_{(x=0)}$  and  $\tau_{g(x=0)}$  are equal to zero. Hence in mathematical terms.

$$T_{(x=0)} = 0 \quad (38a)$$

$$\left( \frac{dT}{dx} \right)_{(x=0)} = 0 \quad (38b)$$

At the same cross-section  $x=0$ , the bending moment at the top lamella is equal to zero, as a free edge. Also, since  $\tau_{(x=0)}$  for the top lamella is equal to zero at  $x=0$ , we can write the following

Mathematical condition:

$$M_{(x=0)} = 0 \quad (38c)$$

$$\left( \frac{dM}{dx} \right)_{(x=0)} = 0 \quad (38d)$$

Having obtained the solutions for  $T_{(x)}$  and  $M_{(x)}$ , the required stresses in the top lamella, glue layer and main beam can be uniquely calculated.

### Numerical Example in connection with the theory

The reinforced beam to be numerically examined is shown in fig. 1,2,3 and 4 with indicated dimensions. The material used for the main beam is dural aluminum with modulus of elasticity  $E = 70GPa$  and Poisson's ratio of  $\nu = 0.33$ . The epoxy resin used for gluing the top lamella with the main beam is with modulus of elasticity

$E_g \cong 5GPa$  and shear modulus  $G_g = \frac{1}{3} E_g$

$$T_{(x)} = Ae^{-\lambda_1 x} + Be^{-\lambda_2 x} + e^{-\lambda_3 x} (C \cos \omega_3 x + D \sin \omega_3 x) + 8.27448 * 10^{-2} M_0$$

$$M_{(x)} = Ame^{-\lambda_1 x} + Bne^{-\lambda_2 x} + 1.629822 * 10^{-3} M_0 +$$

$$+ e^{-\lambda_3 x} [(MC - ND) \cos \omega_3 x + (NC + MD) \sin \omega_3 x]$$

.The main beam is with dimensions: length  $L = 400$  cm, thickness  $H = 10$  cm and width  $b = 2.5$  cm. The glue layer is with dimensions: thickness  $h = 0.1$  cm, length  $l = 100$  cm and width  $b = 2.5$  cm. The reinforcing top lamella is made of steel material with modulus of elasticity  $E_s = 210GPa$  and Poisson's ratio of  $\nu = 0.3$ . The dimensions of the reinforcing lamella are: length  $l = 100$  cm, thickness

$t = 1$  cm and width  $b = 2.5$  cm. Based on the above data, the following values for the eigen values and vectors are obtained.

Eigen values are:

$$\lambda_1 = 4.429339 * 10^{-1} \text{ 1/cm}$$

$$\lambda_2 = 5.390769 * 10^{-1} \text{ 1/cm}$$

$$\lambda_3 = 1.103057 \text{ 1/cm}$$

$$\omega_3 = 6.1680596 * 10^{-1} \text{ rad/cm}$$

Eigen vectors calculated are:

$$m = -7.167714 * 10^{-2} \text{ cm}$$

$$n = -1.471425 * 10^{-1} \text{ cm}$$

$$M = -1.770746 \text{ cm}$$

$$N = 4.072375 * 10^{-1} \text{ cm}$$

Satisfying the boundary condition (38a, b, c, d) the following values for the four constants of integration are obtained:

$$A = -4.587894 * 10^{-1} M_0$$

$$B = 3.863103 * 10^{-1} M_0$$

$$C = -1.026565 * 10^{-2} M_0$$

$$D = -1.019127 * 10^{-2} M_0$$

Therefore the expression for  $T_{(x)}$  and  $M_{(x)}$  can be written in the following form:

Now, the bending moment applied to the main beam  $M_0$  depends on the maximum stress  $\sigma_{ap}$  and is given by the relation:

$$M_0 = \frac{H^2}{6} \sigma_{ap} b$$

$$M_0 = 16.666667 \sigma_{ap} * b$$

Hence, the direct stress in the reinforcing top lamella  $\Delta\sigma_{(x)}$  is given by the relation:

$$\Delta\sigma_{(x)} = \frac{T_{(x)}}{A}$$

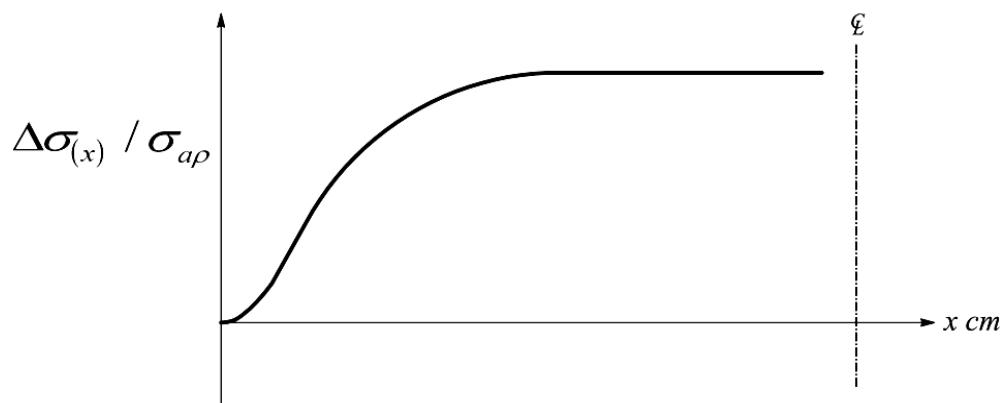


**Figure 5.** Graph of  $\Delta\sigma_{(x)}/\sigma_{ap}$  against  $x$

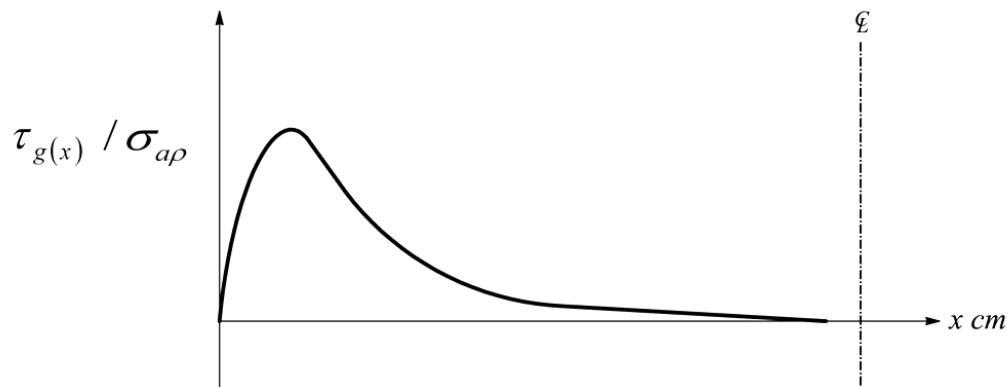


**Figure 6.** Graph of  $\tau_{g(x)}/\sigma_{ap}$  as a function of  $x$

The values for the  $M_{(x)}/\sigma_{ap}$  ratio and  $\sigma_y/\sigma_{ap}$  ratio are tabulated in Table I as a function of the coordinate  $x$ . In fig. 7 is plotted  $M_{(x)}/\sigma_{ap}$  ratio as a function of  $x$ .

The numerical values for  $\Delta\sigma_{(x)}/\sigma_{ap}$  are tabulated in table I as a function of the coordinate  $x$ . The graph of these values is shown in fig. 5.

The numerical values for the shear stress  $\tau_{g(x)}/\sigma_{ap}$  ratio are tabulated in table I also as a function of the coordinate  $x$ .

The graphical representation of these values is shown in fig. 6.

In fig. 8 is presented the  $\sigma_{y(x)}/\sigma_{ap}$  ratio as a dependent variable on the coordinate  $x$ .



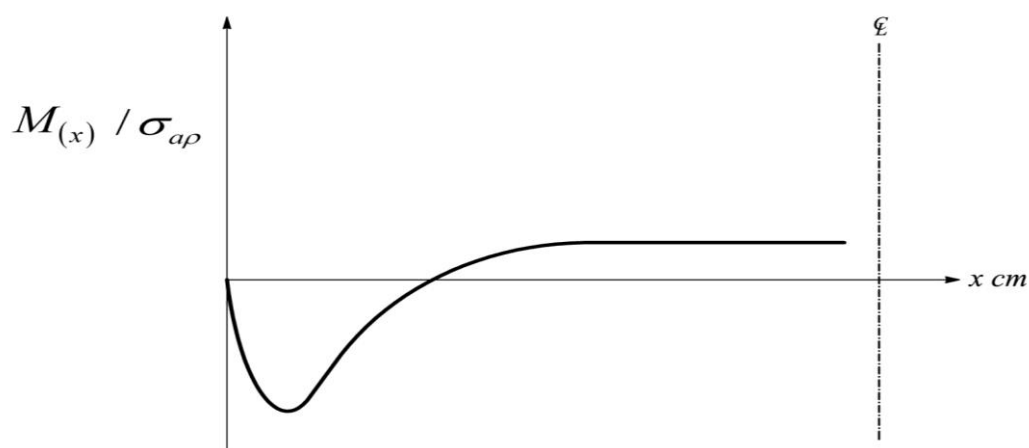


Figure 7. Graph of  $M(x) / \sigma_{ap}$  ratio against  $x$

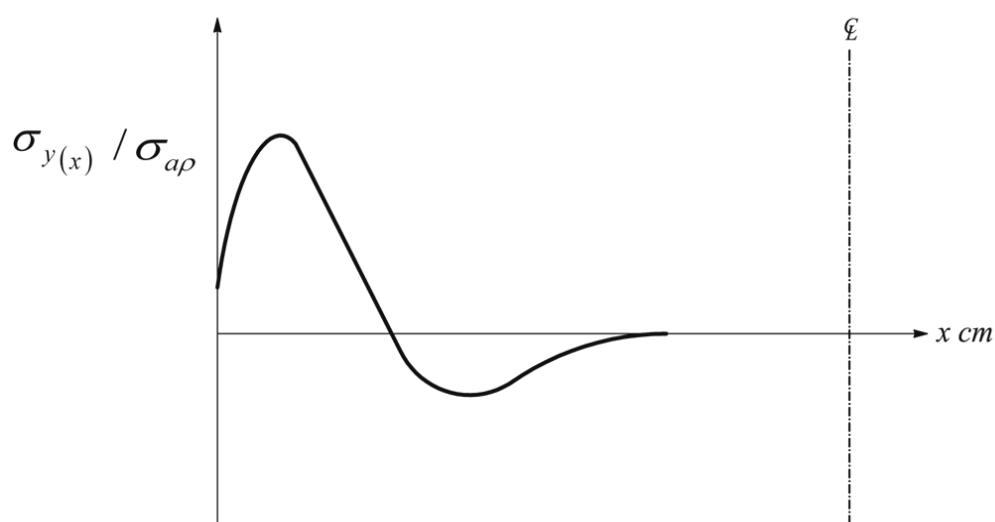


Figure 8.  $\sigma_{y(x)} / \sigma_{ap}$  ratio as a dependent variable on the coordinate  $x$

Table 1. Numerical values for the internal variables

$x$ cm	$\Delta\sigma / \sigma_{ap}$	$M / \sigma_{ap} \text{ cm}^3$	$\tau / \sigma_{ap}$	$\sigma_y / \sigma_{ap}$
0.00	0.00	0.00	0.00	$5.843 * 10^{-2}$
0.25	$1.272 * 10^{-2}$	$-4.103 * 10^{-3}$	$9.574 * 10^{-2}$	$9.206 * 10^{-2}$
0.50	$4.530 * 10^{-2}$	$-1.251 * 10^{-2}$	$1.606 * 10^{-1}$	$1.013 * 10^{-1}$
0.75	$9.114 * 10^{-2}$	$-2.129 * 10^{-2}$	$2.030 * 10^{-1}$	$9.562 * 10^{-2}$
1.00	$1.455 * 10^{-1}$	$-2.838 * 10^{-2}$	$2.293 * 10^{-1}$	$8.184 * 10^{-2}$
1.50	$2.669 * 10^{-1}$	$-3.475 * 10^{-2}$	$2.510 * 10^{-1}$	$4.636 * 10^{-2}$
2.00	$3.926 * 10^{-1}$	$-3.158 * 10^{-2}$	$2.492 * 10^{-1}$	$1.438 * 10^{-2}$
2.50	$5.143 * 10^{-1}$	$-2.256 * 10^{-2}$	$2.360 * 10^{-1}$	$-8.219 * 10^{-3}$
3.00	$6.278 * 10^{-1}$	$-1.135 * 10^{-2}$	$2.175 * 10^{-1}$	$-2.155 * 10^{-2}$

3.50	$7.314 * 10^{-1}$	$-4.222 * 10^{-4}$	$1.968 * 10^{-1}$	$-2.779 * 10^{-2}$
4.00	$8.245 * 10^{-1}$	$8.922 * 10^{-3}$	$1.756 * 10^{-1}$	$-2.935 * 10^{-2}$
5.00	$9.795 * 10^{-1}$	$2.160 * 10^{-2}$	$1.352 * 10^{-1}$	$-2.563 * 10^{-2}$
6.00	1.097	$2.770 * 10^{-2}$	$1.005 * 10^{-1}$	$-1.946 * 10^{-2}$
7.00	1.183	$2.992 * 10^{-2}$	$7.263 * 10^{-2}$	$-1.398 * 10^{-2}$
8.00	1.244	$3.030 * 10^{-2}$	$5.138 * 10^{-2}$	$-9.804 * 10^{-3}$
9.00	1.287	$2.994 * 10^{-2}$	$3.575 * 10^{-2}$	$-6.785 * 10^{-3}$
10.00	1.317	$2.939 * 10^{-2}$	$2.456 * 10^{-2}$	$-4.652 * 10^{-3}$
12.00	1.351	$2.839 * 10^{-2}$	$1.127 * 10^{-2}$	$-2.134 * 10^{-3}$
14.00	1.367	$2.777 * 10^{-2}$	$5.035 * 10^{-3}$	$-9.542 * 10^{-4}$
16.00	1.374	$2.745 * 10^{-2}$	$2.208 * 10^{-3}$	$-4.186 * 10^{-4}$
25.00	1.379	$2.717 * 10^{-2}$	$4.770 * 10^{-5}$	$-9.047 * 10^{-6}$

## CONCLUSION

From the performed numerical calculations on the particular example, the following conclusion are made. The shear stress  $\tau_g$  in the glue layer possesses concentration of its value. It reaches maximum value at distance  $x \approx 1.731 \text{ cm}$ , from the free edge  $x=0$ . Its value is approximately  $0.251 \sigma_{ap}$ . Therefore the maximum value depends on the applied load as well. For dural aluminium the ultimate value is  $510 \text{ MPa}$  which is very large, thus the glue layer is subjected to very large shear stress at that cross-section. It depends on the epoxy raisin whether it can take this shear stress.

Second important stress is the  $\sigma_{yg}$  direct stress in the glue layer. The calculations show that stress concentration takes place as well. The maximum value of this stress takes place near to the free edge, i.e. at  $x=0.539 \text{ cm}$ . Its value is considerably lower then the shear stress maximum, and it is  $\sigma_{yg} \approx 0.101 \sigma_{ap}$ . Again for dural aluminium, it can be very large tensile stress in the glue layer.

On the other hand the direct stress  $\sigma_x$  in the reinforcing lamella is above the maximum value of  $\sigma_{ap}$  for the part of the length. The main conclusion is that the connection strongly depends on the glue characteristics for allowable shear and direct tensile stresses.

This theory can be applied to beams made of concrete and reinforced by fiber Reinforced Polymer (FRP) with great accuracy. The theoretical derivations include the  $\sigma_y$  direct stress in the analysis. Therefore it can be concluded, that near the surface of the connection between the FRP and the concrete beam, considerable  $\sigma_y$  direct stress can develops. If it is tensile, the failure-cracks can take place in the concrete and debonding of the FRP lamella will occur [1,3].

As far as the direct stress  $\sigma_x$  in the glue layer is concern, further analysis in part II will be given.

## SUMMARY

In this paper is analyzed the internal stress state of reinforced beam, subjected to external load.

The reinforced beam analyzed consist of top reinforcing lamella glued on the main beam with epoxy raisin. This connection has geometrical discontinuity in the lengthwise cross-sectional area. Therefore diffusion of stresses is expected in the top lamella, main beam and glue layer. This diffusion of stresses is characterized by concentration of stresses in the top lamella, glue layer and main beam. The main interest of analysis in this paper is the estimate of these stress concentrations, specially shear stress concentration in the glue layer and direct

stress  $\sigma_y$  concentration. For the purpose of the analysis, expressions for internal stresses  $\tau$ ,  $\sigma_x$  and  $\sigma_y$  are derived for the three distinct elements.

Certainly for deriving these expressions, the equations for plane stress equilibrium are used. After that, the generalized equations of compatibility are derived, by making use of the principal of minimum complimentary virtual strain energy. System of two differential equations of generalized compatibility is derived. They are solved in close analytical form. Using the obtained theoretical solution, numerical values are obtained for  $\tau_g/\sigma_{ap}$ ,  $\sigma_{yg}/\sigma_{ap}$ ,  $\Delta\sigma_x/\sigma_{ap}$  and  $M/\sigma_{ap}$ . They are tabulated in table 1.

## REFERENCES

- [1] BALÁZS, L.G. "POTENTIALS IN USE OF EBR AND NSM STRENGTHNING METHODS FOR CONCRETE STRUCTURES". SCIENTIFIC JOURNAL OF CIVIL ENGINEERING, VOLUME 3, NUMBER 1, JULY 2014, SKOPJE
- [2] HURTY, C.W. and RUBINSTEIN, F.M. DINAMICS OF STRUCTURES, PRENTICE-HALL, Inc. ENGLEWOOD CLIFFS, NEW JERSEY 1964
- [3] MEGSON, T.H.G. AIRCRAFT STRUCTURES FOR ENGINEERING STUDENTS, Edward Arnold Ltd. LONDON 1977
- [4] MIHAJLOV, R.M. CONTRIBUTION TO THE ANALYSIS OF AXIAL VIBRATIONS, PROCEEDINGS, G-th SYMPOSIUM ON THEORETICAL AND APPLIED MECHANICS, STRUGA 1998
- [5] MIHAJLOV, R.M. STREES ANALYSIS OF BOOMS-PANEL COMBINATION STRUCTURE, SCIENTIFIC JOURNAL OF CIVIL ENGIENERING, VOLUME 3, NUMBER 1, JULY 2014, SKOPJE
- [6] PRZEMIENIECKI, S.J. THEORY OF MATRIX STRUCTURAL ANALYSIS, McGRAW-HILL BOOK COMPANY, 1968
- [7] SERAFIMOV, P. OSNOVI NA TEORIJATA NA KONSTRUKCIITE I, OPREDELENI
- [8] NOSAČI, MAKEDONSKA KNIGA, SKOPJE, 1984

## Acknowledgment

The author would like to thanks Professor Elena Dumova-Jovanovska, Professor Stanislav Milovanovic and Professor Gorgi Kokalanov for reading the manuscript. Also the author is thanks full to dipl. ing – Architect Stojan Mihajlov for technical preparations of this paper, and assistant Mr. Kristina Manevska for checking related calculations.





**ЖИКОЛ**

**Градете ја Вашата иднина денес.**

...од **1987** година  
традежници прег сè

[www.zikol.com.mk](http://www.zikol.com.mk)



## **CADASTRE SERVICES ORIENTED TOWARD ADMINISTERING WITH AGRICULTURE LAND CONCESSIONS**

### **AUTHORS**

#### **Gjorgjiev Vanco**

Ph.D. Professor

Ss. Cyril and Methodius University

Faculty of Civil Engineering – Skopje

[vanco@t-home.mk](mailto:vanco@t-home.mk)

#### **Gjorgjiev Gjorgji**

Ph.D. Assistant

Ss. Cyril and Methodius University

Faculty of Civil Engineering – Skopje

[gorgi.gorgiev@gmail.com](mailto:gorgi.gorgiev@gmail.com)

The purpose of this paper is to present the status and condition of administered concessions of the state owned agricultural land in one, randomly selected, cadastre municipality (CM).

The paper is focused in all segments of the process of concession administration, from the presentation of the current status in the selected CM, to the real life problems that the concession administration faces in the process of concession approval and management of the concessions.

Based on the conclusions derived from the performed research, this paper in the final part provides certain suggestions and recommendations.

The documentation utilized in preparation of this paper are: national strategy for agricultural and rural development for the period of 2007-2013, Skopje, June 2007, Law for the agricultural land, Agricultural census 2007, Law on the real estate cadaster, Law on concessions.

This paper is based on data for the real estate in the CM of Zubovce, obtained from the real estate cadastre, regional office in Kumanovo, data from the regional office of the Ministry of agriculture, forestry and water management in Kumanovo and direct field observation.

**Keywords:** Agriculture land, cadaster, concession

### **CADASTRE MUNICIPALITY ZUBOVCE**

Cadastre municipality Zubovce is within the administrative borders of the Municipality Klecevce. Zubovce is populated area with 57 inhabitants, in accordance with the census from 2002, and the whole population is with Macedonian ethnicity, consists of 33 families/households and 70 homes / houses. In accordance with the census from 1994, Zubovce had a population of 98 inhabitants, all with Macedonian ethnicity, 49 man and 49 women, 50 households and 76 homes / houses. In accordance with the statistical

data, even though it has a small number of population, the population decreased for 58%, which demonstrates the tendency of depopulation of the rural areas in the state.

The total area of the cadastre municipality is 7,971,748 m<sup>2</sup>, where 4,134,227 m<sup>2</sup> (51.86%) of the total area is state owned land and 3,837,521 m<sup>2</sup> is privately owned land, or 48.14% of the total area.

## **CONCESSIONS AND THEIR RELATION TO THE REAL ESTATE REGISTRY SYSTEM**

In accordance with the Law on concessions, the Government of the Republic of Macedonia can approve state owned agricultural land to be operated under concession to a domestic and foreign legal and physical entity. The concession can be approved for the following exploitation:

- Production for livestock fodder and development of the livestock production for a period of 20 to 30 years.
- Crop production for a period of 20 to 30 years
- Green-house production for a period of 30 to 40 years
- Permanent crop for a period of 30 to 40 years
- Land for growing of wild animals and aquaculture production for a period of 10 to 30 years, unless otherwise regulated with another law.

The concession of the agricultural land is approved on the basis of implemented public request for proposals, based on the information for the real estate property (state owned agricultural land), the initial amount of concession fee, and the requirements for a Program for the exploitation of the agricultural land. The technical and administrative activities for releasing of the agricultural land for concessional use, is performed by the Ministry of Agriculture, forestry and water management. In accordance with the decision for releasing of the agricultural land for concession, the Minister of Agriculture, forestry and water management signs the Concession Agreement in written form with the company that has submitted the best offer, on behalf of the Government of Republic of Macedonia.

What data is used as a base within the process of concession administration? One of the key preconditions for start with the process of administration of land of concession or lease, is the data of spatial distribution of the agricultural land, its soil quality and its type of use. This is the area where, in the process of concession administration, most of the problems and misunderstandings occur.

In accordance with the institutional position of the state real-estate registry, the required data are obtained from the Real-estate cadastre form the State department for geodetic works. The data obtained from this system, not only satisfies the requirements with content data in the process of concession, they are also the sole data possessing the legality.

Where are the defects of this system, often criticized for its lack of data of the current situation and conditions of the real-estate, especially in the case of agricultural land in state ownership?

Neglect and the insufficient knowledge of the legal jurisdiction which is base for the process of land registration can create problems. For instance, obligation and jurisdiction for registration of the legal and ownership status of the real estate, initiated outside the system, has no obligation to follow the principle of current condition by either form or quantity of data.

Having in mind the stated above, it is obvious that the process of concession can not be performed based on only that data and it is real to expect, especially from the potential concession holders, to additionally hire legal experts and private geodetical companies to record the real current status of the agricultural land for which they have applied for and/or was approved for concessional use to them.

## **THE LAND STRUCTURE IN CADASTRE MUNICIPALITY ZUBOVCE**

The state-owned agriculture land in Zubovce has suitable structure for concession, based on the soil quality, type of use and the high level of the land parcels grouping. Ownership registration of this land is based on the Law on Real Estate Cadastre where the land of interest, state-owned agriculture land, is grouped in the following ownership lists: 42, 113, 130, 198, 334, 355 и 356. These data are

provided from the regional office of the State Department for Geodetic Works in Kumanovo.

Total area available for the concession process, based on the type of use and land category, for the CO Zubovce is presented in the table below: It is evident that, from the total area of state owned land (4,134,227 m<sup>2</sup>) in

Zubovce, the area of attractive agriculture land available for concession is 3,435,935 m<sup>2</sup>. The difference of 698,292 m<sup>2</sup> belongs to rivers and roads, which is not attractive for the concession process. This relationship is presented in the Figures 1, below.

Type of use ID	Type of use description	Area (m <sup>2</sup> )
110	Fields	1,287,463
140	Vineyards	29,695
150	Meadow	6,291
160	Pastures	2,072,742
170	Forest	39,644
<b>Total area:</b>		<b>3,435,935</b>



Figure 1.

## STATUS OF ISSUED CONCESSION

In accordance with the performed analyses of the documentation and the registry system of concessions at the regional unit of the Ministry of Agriculture, Forestry and Water Management in Kumanovo, two subsequent concession procedures for the state owned agricultural land in Zubovce can be observed.

### First line of concessions

The concession was with following parameters:

- 61 land parcels have been administered covering a total area of 172,726 m<sup>2</sup>

Type of use ID	Type of use description	Area (Ha)	Area (ari)	Area (m <sup>2</sup> )
110	Field	14	29	25
140	Vineyards		7	12
160	Pastures	2	89	19
170	Forest		1	70
<b>Total area:</b>		<b>17</b>	<b>27</b>	<b>26</b>

- The land parcels comprises of fields (type of use code: 110), pastures (type of use code: 160), vineyards (type of use code: 170) and forest (type of use code: 140)

The total area per type of use and land class is represented in the table bellow, while the land mapping is presented at Figure 2.

There is no detailed information regarding this line of concession at the regional office of the Ministry of agriculture, forestry and water management. There is evidence about paid/not pad annual concession fees, without clear clarification and confirmation about concessionaire practice on the field, as well as the level of utilization of all parcels and related objects.

### Second line of concessions

The concession was with the following parameters:

- 100 land parcels have been administered with a total area of 338,386 m<sup>2</sup>

Type of use ID	Type of use description	Area (Ha)	Area (ari)	Area (m <sup>2</sup> )
110	Fields	30	50	70
140	Vineyards		19	83
160	Pastures	2	95	33
150	Meadows		18	00
<b>Total area:</b>		<b>33</b>	<b>83</b>	<b>86</b>

- The land parcels comprised of fields (type of use code: 110), pastures (type of use code: 160), meadows (type of use code: 150) and vineyards (type of use code: 140)

The total area per type of use and land class is represented in the table bellow, while the land mapping is presented at Figure 3.

This concession was approved to one legal entity – Agrokonzum. The concessionaire, after signing the Concession Agreement is in the phase to determine the current condition on the field.

For this purpose the concessionaire has hired private geodetical company to prepare geodetic project for the land which was approved under concession.

There are no other field activates.





Figure 2. First line of concessions

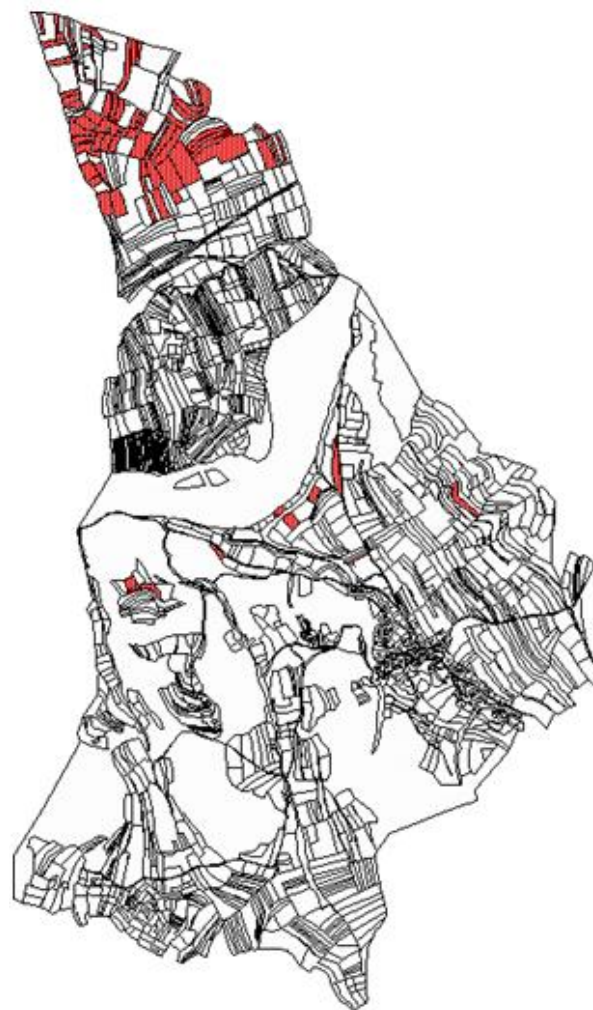


Figure 3. Second line of concessions

### Analyses of the actual field situation with the administered concessions contained

Even though there is no evidence within the responsible institutions, there are a number of problems that both lines of concessions faced in the process of implementation of the concession on the field. These problems are typical for all agricultural land in the Country, but are more common on the state-owned land. The background situations for these problems can be grouped into four categories:

1. Arondation is a process for exchange of land among two parties, where in this case are the state and other physical and/or legal entities, performed for various interests and reasons. The mutual obligations are regulated with agreements that do not end at the real-estate cadastre, which

on the other side provides data for concession issuance.

2. Land usurpation

Land usurpation is an exploitation of land that belongs to somebody else, in this case the land is state-owned, which in many instances in this country is concluded by the state (i.e. the agricultural combines, which use those lands) where with different motives, the state made no corrective activities.

3. Conflicts among the legal regulative which occur in appropriate time intervals. In this category a lot of legal regulative belong such as Law on the agrar reform and colonization, Law on nationalization, Arondation steps, Law on expropriation, Law on spatial and urban planning, Construction law, Law on constructional sites, Law of



denationalization, Law on privatization of the private construction site in state ownership.

All those regulative resulted into certain legal activities, which in time were amended, supplemented, terminated or have generated different legal activities.

#### 4. Uncompleted administrative procedure

This group comprises of activities with the land that are regulated with legal acts and procedures, but have not resulted with recording of the changes within the real estate cadastre, due to various reasons.

These situations will be presented by the analyses of the land parcel's geometrical forms and type of use provided by the real estate cadastre and the same areas as seen on the field. Not all cases need to be real problems in the process of concession administration, but without clear verification before the concession starts there are possibilities for problems occurrence.

Aerial orthophotos from the State Department of Geodesy will be used for the presentation of the field situation.

## Case 1

Part of the data from the first line of concessions is presented on the Figure 4. It is evident that real estate cadastre data used for the concession administration is not updated with the current state of the land. It is visible on the Figure that land parcels 1693, 1697, 1698, 1699, 1703 and 1717, which are subject of concession, are not updated with the new roads which take out part of its areas. It should be noted that the concessionaire is paying the fee based on the cadastre data, which is more that he is practicing on the field.

The possible scenarios for this case are:

1. The roads are built by municipality administration. This is the most probable scenario since the road is about 3.5 meters wide and spreads on the whole CM. But, here is the 4th situation, where these changes are not updated in the real estate cadastre.
2. The roads are built by the land owners in order to establish access to its own parcels. Even in this case, there is 4th situation, where these changes should be updated in the real estate cadastre for each parcel separately.

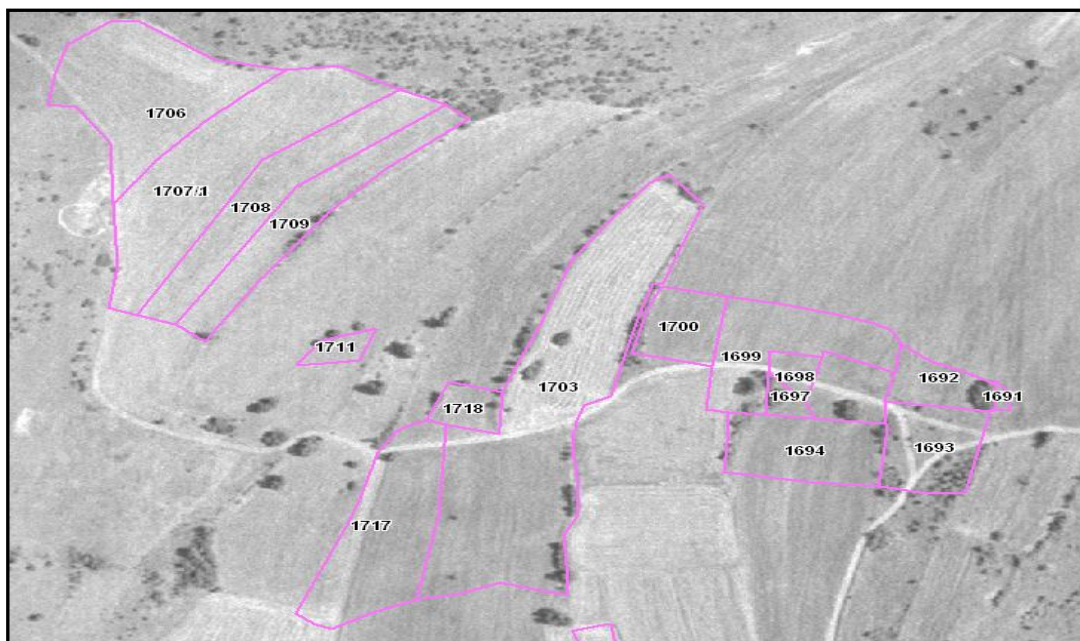


Figure 4.

## Case 2

Land parcels No 106 and 119, subject of the second line of concessions, in the real estate cadastre are registered with coownership between state and private ownership.

According to the property lists No 355 and 354, these two land parcels have the following ownership:

Land parcel number	State owned	Privately owned	No. of Private entities
106	103 / 118	15/118	3
119	1 / 167	166 / 167	7

In addition, each of the land parcels have the same type of use (fields), but 2 soil types, which is registered in the cadastre and visible

on the field – Figure 5. Spatially, land parcels are correct comparing the cadastre data and on-the-field situation.



Figure 5.

Having in mind that these two parcels are part of the second line of concession in this municipality, the legal obligation is all owners to provide written agreement for it.

The possible scenarios for this case are:

1. Land ownership is registered in the real estate cadastre, but there is possible legal discrepancy, most probably between the Law on Concession and Law on Ownership and other real property deeds.
2. There is regular documentation which was not available during the period of paper preparation.

## Case 3

The Figure 6 shows a situation of land usurpation, quite interesting for a parcel in a

state ownership. It is evident that the parcel 19 with its shape and the area position registered at the real estate cadastre is different from the situation on the field. The parcel's boarder on one side is marked alongside the road, where the usurpation from the parcels 34, 33 and 32 forms new road and a new shape of the parcel 19. The parcel 19 in the second phase concession is marked with the figure registered in the cadastre, and the concessionaire will have more land for cultivation.

The possible scenarios for this case are:

1. This is typical case for land usurpation, which is strange looking from the point that the state land is expanded on the account of privately owned land. It leads to the possibility



that this parcel is used by some private entity.



Figure 6.

#### Case 4

The Figure 7 shows the increase of the parcels 7, 19 and 36 derived by a similar motive for usurpation as it was the case in the previous figure. The type of interventions that have occurred can be verified by legal and technical documentation, provided that such documentation exists. The cadastre municipality was not in a position to provide any documentation; with an explanation that documentation of that kind does not exist within the appropriate institutions.

#### Case 5

Figure 8 shows a situation of completely altered situation of the parcel's shapes of 42, 43 and 44. We can note that the current condition of the parcel's shape of the whole area is completely different compared to the situation registered with the real estate registry.

There are many scenarios for this case that belongs to the all 4 situations that have been specified as reasons for problems in the process of concession administration.



Figure 7.



Figure 8.

### Case 6

Figure 9 presents a situation where the current field condition and the situation obtained from the registry are identical and can be

overlapped. We can note that the parcel 113 cultivates two crops, which overlaps with the situation recorded within the database of the real estate registry.

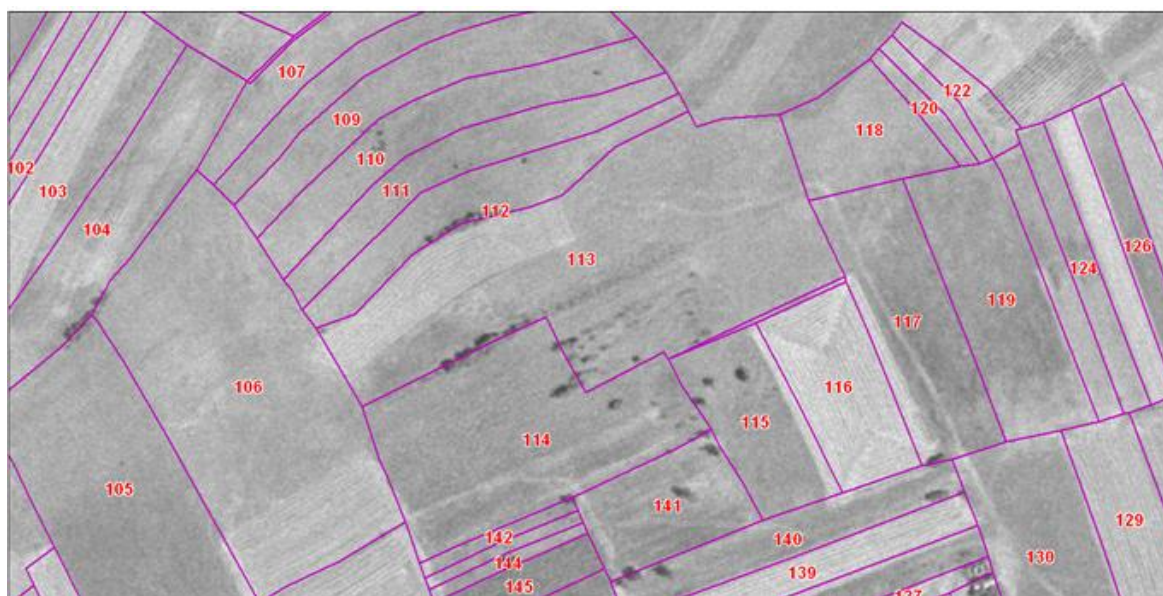


Figure 9.

## CONCLUSIONS AND RECOMMENDATIONS

In order to confirm the current situation on the field, as well the situation registered with the registry system, which have been used for concession purposes, the general conclusions

based on the performed comparative analysis of the field, acquired with additional geodetic acquisition methods, are:

- Additional acquisition methods need to be employed and geodetical projects have to be prepared based on

- the results of the acquisition, in the preparatory phase
- The data obtained by the performed geodetic activities, should be integrated within the existing geometric database for the cadastral municipality
  - Legal documentation needs to be determined and provided to resolve the ownership issues of the current situation on the field
  - Develop a unique system for registry and administration of the state owned agricultural land
  - Development of an infrastructure for data distribution and marketing of the agricultural land



## PREPARATION OF LANDSLIDE SUSCEPTIBILITY MAPS USING GIS, RECENT CASE STUDY IN R.MACEDONIA

### AUTHORS

#### **Igor Peševski**

Ph.D. Associate Professor  
University "Ss. Cyril and Methodius"  
Faculty of Civil Engineering – Skopje  
[pesevski@gf.ukim.edu.mk](mailto:pesevski@gf.ukim.edu.mk)

#### **Milorad Jovanovski**

Ph.D. Professor  
University "Ss. Cyril and Methodius"  
Faculty of Civil Engineering – Skopje  
[jovanovski@gf.ukim.edu.mk](mailto:jovanovski@gf.ukim.edu.mk)

#### **Jovan Br. Papić**

Ph.D. Associate Professor  
University "Ss. Cyril and Methodius"  
Faculty of Civil Engineering – Skopje  
[papic@gf.ukim.edu.mk](mailto:papic@gf.ukim.edu.mk)

#### **Luka Jovičić**

MSc in Engineering Management  
GIS Consultant  
[jovicic.luka@gmail.com](mailto:jovicic.luka@gmail.com)

GIS landslide inventory and susceptibility maps are the first step towards detection of future landslides. In recent years, some efforts are made to prepare such maps for the territory or parts of the territory of Macedonia. This paper presents use of GIS for one attempt method, by the so called arbitrary – polynomial method which was applied on the territory of Polog-Reka. In order to prepare susceptibility map following this method, thematic maps were first found in the literature and from different sources and archives. Processed from different sources, formats, quality and scale, map layers were saved as vector and raster datasets depending whether they represent discrete or continual data. After this, so called rating maps were calculated upon which the final susceptibility map could be derived. Main problems during preparation of maps were data/thematic map accessibility, datasets accuracy, details, currency, resolution, etc. However, using the tools which the GIS provides, datasets were processed in structure that enables seamless analysis and use. Also, the GIS approach enabled stored datasets and results to be viewed, analyzed and updated in standardized and interoperable manner. Statistical data analysis as one of the most important aspects in landslide susceptibility was performed in required way enabling flexible factors, formulas and analysis change.

**Keywords:** landslide susceptibility, thematic maps, preparation, GIS tools

### INTRODUCTION

Use of Geographic Information System (GIS) techniques in landslide inventory, monitoring, hazard and risk mapping/zoning is increasing fast worldwide. Most important papers in this field are written by Brabb E.E. (1984); Soeters R. et al. (1991); Westen Van C.J. et al. (1993); Carrara, A, et al. (1995); Soeters R. & Westen Van C.J (1996); Huabin W. et al. (2005); Cascini. L et al. (2005); Fell R. et al. (2005); Chacon et al. (2006).

In recent years, efforts are made to prepare such maps for the whole or parts of the

territory of Macedonia with relatively good results (Milevski et al.2010, Jovanovski et al. 2011).

Following these positive examples, here we present the process of preparation of GIS landslide inventory and susceptibility maps for the Polog – Reka region in Republic of Macedonia.

This region is selected as most interesting, as previous studies have shown that most landslides in Macedonia occur within its frames. (Jovanovski et al. 2011).

## LANDSLIDE INVENTORY MAP

Necessary basis for enabling preparation of landslide susceptibility, hazard and risk maps is the landslide inventory map of an area. For our example, the landslide inventory map was created using data from the following sources and formats; some of the problems during data transfer and processing into GIS are noted:

- Basic Geological Map of the Republic of Macedonia, sheets Gostivar, Kicevo, Skopje, Prizren, Krushevo in scale 1:100000. Source: jpeg. scan of the Basic Geological map of Macedonia (slight deformations of the scanned analogue maps, corrected in GIS).
- Topographic maps in scale 1:25000, taken from the DEM of Republic of Macedonia (downscaled in GIS to scale 1:100000).
- Engineering geological maps, sheets Gostivar and Kicevo, scale 1:100000, (dwg format, difficulties when transferring into GIS shapefile, geological borders had to be redrawn)
- Google earth and Google maps applications (precision is lower and used as informative data.
- GIS – portal of the Agency for Real Estate
- Orthophoto images in scale 1:5000 available from GIS portal of the Agency for Real estate).
- Topographic and situation maps of larger formerly registered landslides. (various coordinate systems, needed transformations were performed by the GIS tools).

Using all these sources, 1172 landslides were identified. Resulting GIS landslide inventory map is presented on fig. 1. It should be stated that detected landslides according Cruden and Varnes (1996) classification fall into one of the following groups: rockfall, rock slide, debris

flow, rotational/translational rock slides, rock spread.

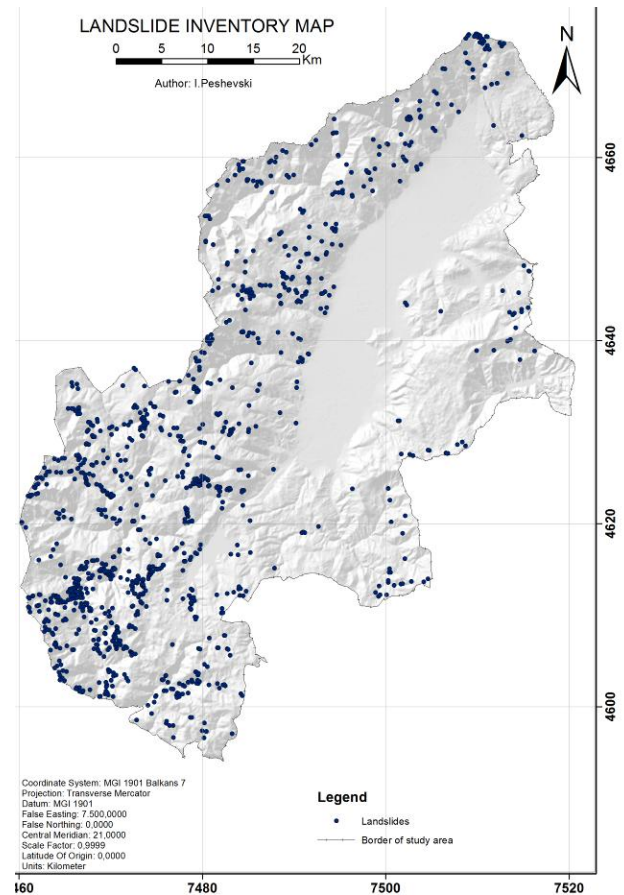


Figure 1. Landslide inventory map of the study area

## THE ARBITRARY POLYNOMIAL METHOD

From the obtained landslide inventory map of the region, it is relatively obvious (first approximation) where future landslides have to be expected. For further confirmation of this statement, susceptibility assessment with the so called arbitrary polynomial method was performed.

The method is based on gradation (rating) of landslide casual factors according their importance for landslide development. Details for the method are presented in Jovanovski M. et al. (2011), and Peshevski I. (2015). Most important to mention for this method is that gradation – ratings are defined semi-empirically, and above all, in dependence of involvement of each casual factor in historical landslide occurrences. According statistical data (Peshevski et al. 2013), as most important landslide factors for the analyzed region, the following were selected: geological composition, slope angle (inclination),

precipitation (rainfall), seismic conditions (intensity), and land use.

Having processed necessary data and created layers showing chosen factors, the landslide casual factors thematic maps were prepared in the GIS environment. Some problems in data transfer were encountered as during preparation of landslide inventory map, but were solved relatively easy using the GIS processing tools. Knowing the character of this paper, thematic maps are not presented and can be found in (Peshevski 2015).

Next step was preparation of rating maps. Rating from 0,1 to 3 was arbitrary assigned to the lithological type and slope inclination (for the latter, rating is performed using polynomial interpolation), 0,1 to 2,0 for precipitation, and 0,1-1 for maximum expected seismic intensity according the MSK-64 scale and land use data (source Corine CLC). Details for ratings of each landslide casual factor are also given in Peshevski 2015, and here only rating maps are presented. Using the structured data in the GIS software, spatial tools were used for preparing rating maps in theoretically referenced methodological way.

For example, the rating maps for lithology, slope inclination and precipitation are presented on following figures 2, 3 and 4.

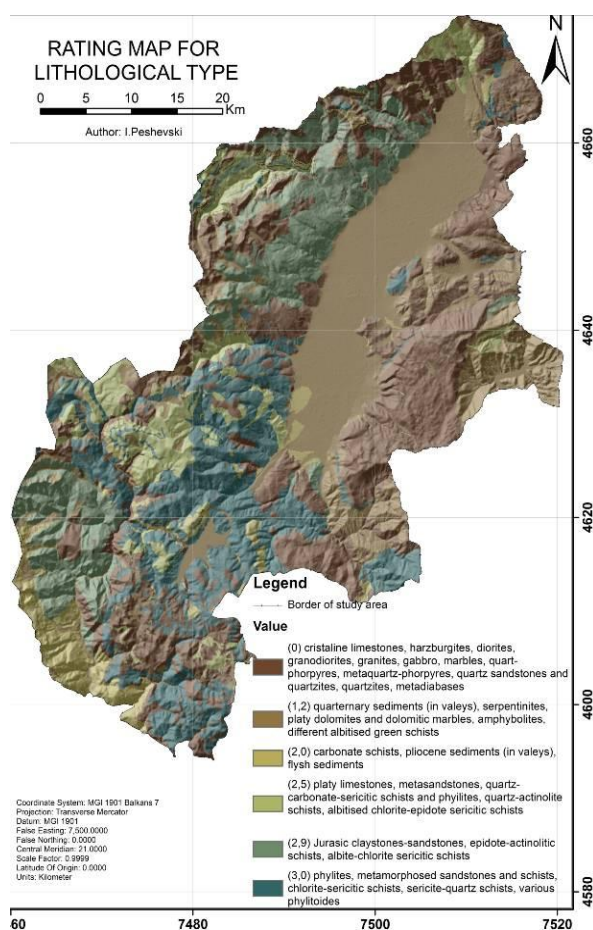


Figure 2. Rating map according lithological type

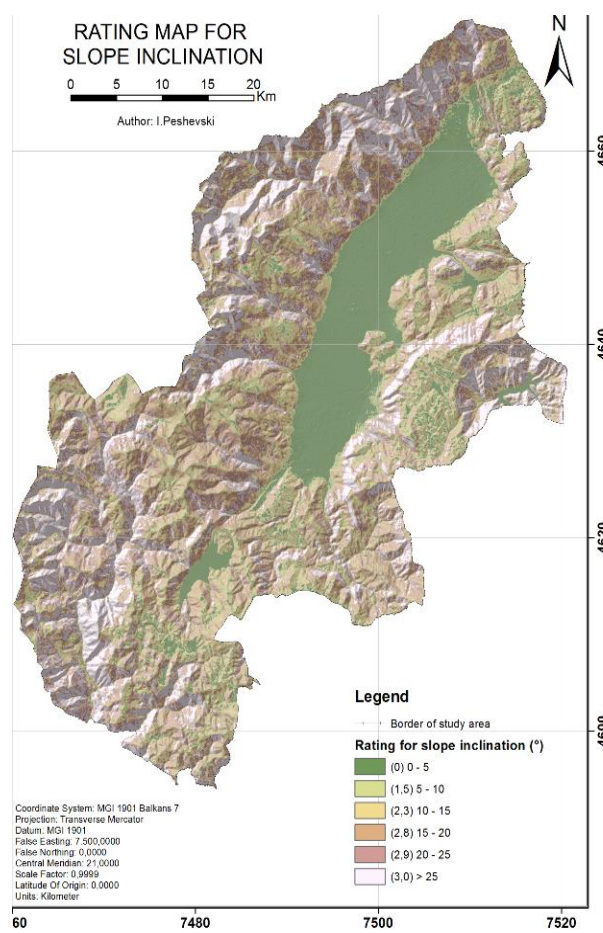


Figure 3. Rating map for slope inclination



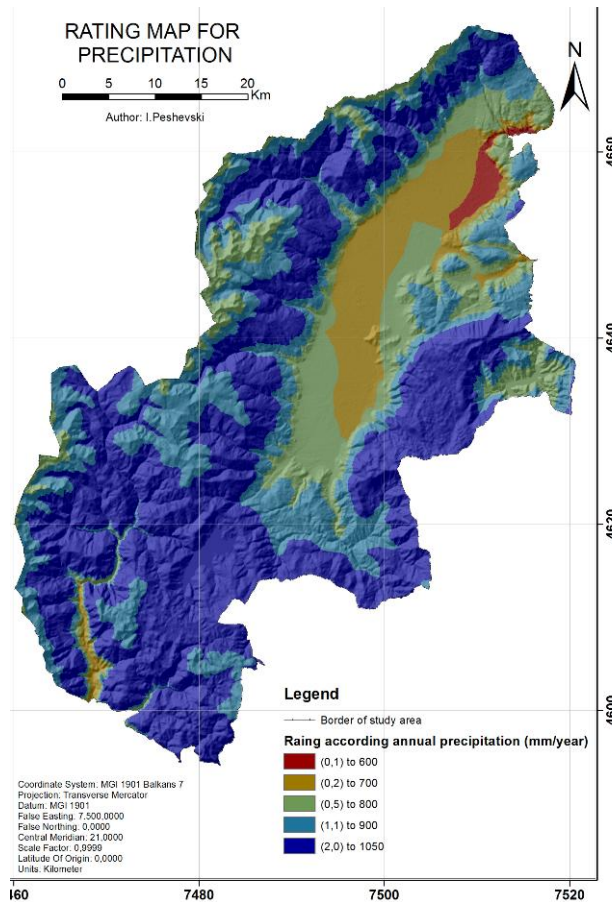


Figure 4. Rating map for precipitation

### LANDSLIDE SUSCEPTIBILITY MAP

Using the geoprocessing tools in the GIS program, and with specific, yet simple mathematical equation, the landslide susceptibility degree throughout the analysed region was obtained. Here it is named Total Landslide Susceptibility Rating (Equation 1).

$$TLSR = LT-R + S-R + P-R + I-R + LU-R \quad [1]$$

where:

TLSR – total landslide susceptibility rating

LT-R – value of rating for lithological type

S-R – value of rating for slope inclination

P-R – value of rating for precipitation

I-R – value of rating for seismic conditions

LU-R – value of rating for land use

As a basic output, the total landslide susceptibility rating was calculated for return period for maximum expected seismic intensity for 100 according the MSK-64 seismic intensity scale. The terrain was then divided into 5 zones of landslide susceptibility by using of mathematical function equal interval. The landslide susceptibility map is obtained, which for the goals of verification was then

overlapped with the landslide inventory map. The resulting susceptibility map is presented on figure 5.

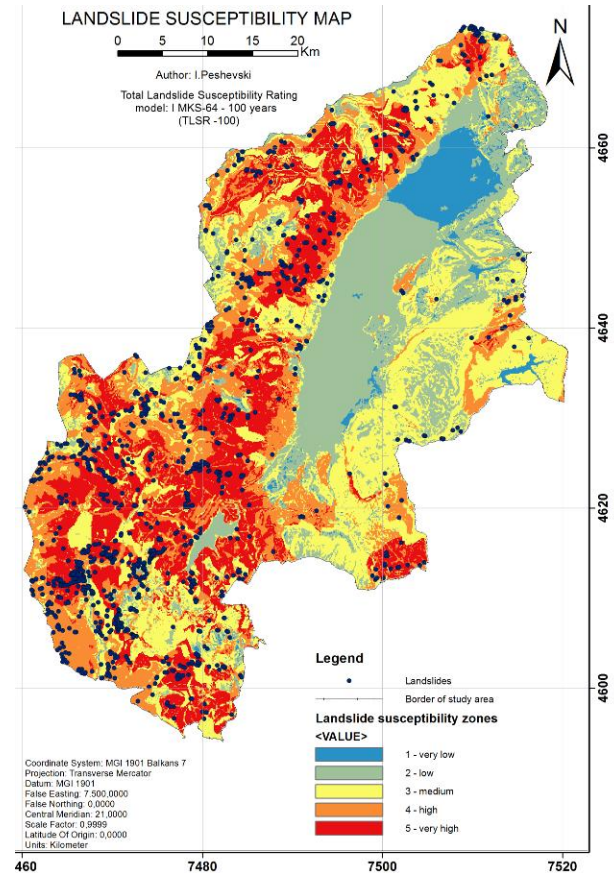


Figure 5. Landslide susceptibility map of study area

Predefined formulas and capabilities of GIS analytical tools enabled verification to be performed very fast. The obtained results are presented on following table 1.

Table 1. Landslide susceptibility classes for return period of maximum expected seismic intensity of 100 years

Landslide susceptibility	TLSR value	area (km <sup>2</sup> )	area (%)	lands-lides	landsli des (%)
<b>1 – very low</b>	0,5-2,3	101	4,17	2	<b>0,17</b>
<b>2 – low</b>	2,3-4,14	508	21,0	24	<b>2,05</b>
<b>3 – medium</b>	4,14-5,9	733	30,3	244	<b>20,82</b>
<b>4 – high</b>	5,9-7,78	538	22,2	323	<b>27,56</b>
<b>5 – very high</b>	7,78-9,6	539	22,2	579	<b>49,4</b>
<b>Total</b>				<b>1172</b>	<b>100</b>

In order to present the possibilities of the GIS program and also test the sensitivity of the arbitrary polynomial model, several versions of the landslide susceptibility map were prepared.

The maps are prepared using the following weighted factors:

- Weighted lithological rating map by factor 0.3 and the rest factors by 0.175

$$\text{WLT-TLSR} = \text{LT-R} \cdot 0.3 + \text{NT-R} \cdot 0.175 + \text{GV-R} \cdot 0.175 + \text{I-R} \cdot 0.175 + \text{ZP-R} \cdot 0.175$$

- Weighted slope inclination rating map by factor 0.3 and the rest factors by 0.175

$$\text{WNT-TLSR} = \text{LT-R} \cdot 0.175 + \text{NT-R} \cdot 0.3 + \text{GV-R} \cdot 0.175 + \text{I-R} \cdot 0.175 + \text{ZP-R} \cdot 0.175$$

- Weighted precipitation rating map by factor 0.3 and the rest factors by 0.175

$$\text{WGV-TLSR} = \text{LT-R} \cdot 0.175 + \text{NT-R} \cdot 0.175$$

$$+ \text{GV-R} \cdot 0.3 + \text{I-R} \cdot 0.175 + \text{ZP-R} \cdot 0.175$$

- Weighted landuse rating map by factor 0.3 and the rest factors by 0.175

$$\text{WZP-TLSR} = \text{LT-R} \cdot 0.175 + \text{NT-R} \cdot 0.175 + \text{GV-R} \cdot 0.175 + \text{I-R} \cdot 0.175 + \text{ZP-R} \cdot 0.3$$

For all these maps, verification was performed as for the basic susceptibility maps and variations in the results were obtained. It should be mentioned that, all prepared maps are for return period of seismic intensity of 100 years according MKS scale. If more conservative approach is applied, then a longer return period, of 500 years can be used instead. Processed results are given in following tables.

**Table 2.** Landslide susceptibility classes of the terrain for weighted lithological type (WLT-TLSR) for return period of maximum expected seismic intensity of 100 years and presence of landslide in each class.

Landslide susceptibility	TLSR value	area (km <sup>2</sup> )	area (%)	landslides	landslides (%)
<b>1 – very low</b>	0,0875-0,481	55.27	<b>2,28</b>	7	<b>0,6</b>
<b>2 – low</b>	0,481-0,8745	763.12	<b>31,52</b>	116	<b>9,9</b>
<b>3 – medium</b>	0,8745-1,268	519.49	<b>21,46</b>	147	<b>12,54</b>
<b>4 – high</b>	1,268-1,6615	443.43	<b>18,32</b>	260	<b>22,18</b>
<b>5 – very high</b>	1,6615-2,055	639.58	<b>26,42</b>	642	<b>54,78</b>
<b>Total</b>		<b>2420.89</b>	<b>100</b>	<b>1172</b>	<b>100</b>

**Table 3.** Landslide susceptibility classes of the terrain for weighted slope angle (WNT-TLSR) for return period of maximum expected seismic intensity of 100 years and presence of landslide in each class.

Landslide susceptibility	TLSR value	area (km <sup>2</sup> )	area (%)	landslides	landslides (%)
<b>1 – very low</b>	0,08749-0,481	250.40	<b>10,34</b>	4	0,34
<b>2 – low</b>	0,481-0,8745	248.08	<b>10,25</b>	7	0,6
<b>3 – medium</b>	0,8745-1,268	554.74	<b>22,91</b>	149	12,71
<b>4 – high</b>	1,268-1,6615	672.28	<b>27,77</b>	325	27,73
<b>5 – very high</b>	1,6615-2,055	695.39	<b>28,72</b>	687	58,62
<b>Total</b>		<b>2420.89</b>	<b>100</b>	<b>1172</b>	<b>100,00</b>

**Table 4.** Landslide susceptibility classes of the terrain for weighted precipitation (WGV-TLSR) for return period of maximum expected seismic intensity of 100 years and presence of landslide in each class.

Landslide susceptibility	TLSR value	area (km <sup>2</sup> )	area (%)	landslides	landslides (%)
<b>1 – very low</b>	0,1-0,466	101.93	<b>4,21</b>	2	<b>0,17</b>
<b>2 – low</b>	0,466-0,832	459.05	<b>18,96</b>	31	<b>2,65</b>
<b>3 – medium</b>	0,832-1,198	689.52	<b>28,48</b>	198	<b>16,89</b>
<b>4 – high</b>	1,198-1,564	591.28	<b>24,42</b>	340	<b>29,01</b>
<b>5 – very high</b>	1,564-1,93	579.11	<b>23,92</b>	601	<b>51,28</b>
<b>Total</b>		<b>2420.89</b>	<b>100</b>	<b>1172</b>	<b>100</b>



**Table 5.** Landslide susceptibility classes of the terrain for weighted land use (WZP-TLSR) for return period of maximum expected seismic intensity of 100 years and presence of landslide in each class.

Landslide susceptibility	TLSR value	area (km <sup>2</sup> )	area (%)	landslides	landslides (%)
<b>1 – very low</b>	0,1-0,4409	50.72	<b>2,1</b>	2	0,17
<b>2 – low</b>	0,4409-0,7819	626.23	<b>25,87</b>	38	3,24
<b>3 – medium</b>	0,7819-1,1229	710.92	<b>29,37</b>	247	21,08
<b>4 – high</b>	1,1229-1,4639	711.64	<b>29,40</b>	404	34,47
<b>5 – very high</b>	1,4639-1,8049	321.38	<b>13,28</b>	481	41,04
<b>Total</b>		<b>2420.89</b>	<b>100</b>	<b>1172</b>	<b>100,00</b>

## CONCLUSION

Presented results show that landslide susceptibility modeling is very sensitive process and greatly depends on the quality and precision of input data, appropriate gradation of landslide casual factors, application of correction factors, mathematical models, borders of the study area, etc.

Therefore, it is very important to collect and keep structured and up-to-date all landslide, geological, meteorological, landuse, seismic and other data into databases. This will enable establishment of powerful mathematical and analytical correlations between occurred landslides and casual factors, which is of essential importance for preparation of best suited landslide susceptibility or hazard maps. This is all achievable if advanced GIS tools are used, if there exist functional landslide database, and of course if experts from different geo-scientific fields are involved.

## REFERENCES

- [1] Brabb, E.E. (1984). Innovative approaches to landslide hazard mapping. Proceedings 4th International Symposium on Landslides, Toronto, 1: 307-323.
- [2] Carrara, A. et al. (1995) GIS technology in mapping landslide hazard. In: Carrara A., Guzzetti F. (Eds.), Geographical Information Systems in Assessing Natural Hazards. Kluwer Academic Publisher, Dordrecht, The Netherlands, 135-176.
- [3] Cascini, L. et al. (2005). Landslide hazard and risk zoning for urban planning and development. In Landslide Risk Management O. Hungr, R. Fell, R. Couture and E. Eberhardt (editors). Taylor and Francis, London. 199-235.
- [4] Chacon J., et al. (2006). Engineering geology maps: landslides and geographical information systems  
Received: 6 June 2005 / Accepted: 24 June 2006 / Published online: 31 October 2006 Springer-Verlag.
- [5] Cruden D.M. и Varnes D.J. (1996). Landslide types and processes. In: Turner A.K.; Shuster R.L. (eds) Landslides: Investigation and Mitigation. Transp Res Board, Spec Rep 247, pp 36–75.
- [6] Fell. R., et al. (2005). A framework for landslide risk assessment and management. Proc. Int. Conf. on Landslide Risk Management, Vancouver, Canada, pp. 3–25.
- [7] Huabin W. et al. (2005). GIS based landslide hazard assessment: an overview, Progress in Physical Geography 29 (4): 548-567.
- [8] Jovanovski M. 2011. Landslides and Rock Fall occurrences and processes in R. Macedonia, Croatia–Japan Projecy on Risk Identification and land-use planning for disaster mitigation of landslides and floods in Croatia, 1st Project workshop „International experience“, Dubrovnik.
- [9] Jovanovski, M., Abolmasov, B. and Peshevski, I. 2011. Analyses of Landslide Hazard Evaluation Factors using polynomial interpolation, Second World Landslide Forum, Rome.
- [10] Milevski, I., Markoski, B., Jovanovski, M. and Gorin, S. 2010. Landslide Risk Mapping by Remote Sensing and GIS in Gevgelija-Valandovo Basin. Geologica Balcanica, No39, Sofia, BAS, pp.255.
- [11] Pesevski I., et al. (2012) Approaches to preparation of national landslide and rockfall database and hazard-risk maps in R.Macedonia, Scientific Journal of

- Civil Engineering, Vol.1, No.1; 12.2012, pp.49-55
- [12] Peshevski I., et all. (2013). Landslide inventory map of the Republic of Macedonia, statistics and description of main historical landslide events, Proceedings of the first regional Symposium on Landslides in the Adriatic-Balkan Region. 6-9 march, 2013, Zagreb, Croatia.
- [13] Peshevski I. (2015). Landslide susceptibility modelling using GIS technology, Phd Thesis, Faculty of Civil Engineering – Skopje.
- [14] Soeters R. et al. (1991). Remote sensing and geographical information systems as applies to mountain hazard analysis and environemntal monitoring. In: 8th thematic conference on geology and remote sensing, Denver, vol. pp.1389-1402.
- [15] Soeters R. и Westen Van C.J. (1996). Slope instability recognition, analysis, and zonation. In: Landslides, investigation and mitigation / ed. by. A.K. Turner and R.L. Schuster. Washington, D.C. National Academy Press, 1996. ISBN 0-309-06151-2. ( Transportation Research Board, National Research Council, Special Report ; 247) pp. 129 – 177.
- [16] Westen Van, C.J., et al. (1993) GISSIZ: training package for geographical information systems in slope instability zonation. ITC publication, vol 15. International Institute for Aerospace and Earth Resources Survey, ITC, Enschede, 245 pp.



**SJCE**

**SCIENTIFIC  
JOURNAL  
OF CIVIL  
ENGINEERING**